Derivation of Class II Force Fields. 7. Nonbonded Force Field Parameters for Organic Compounds

Carl S. Ewig,* Thomas S. Thacher,† and Arnold T. Hagler*,‡

Molecular Simulations Inc., 9685 Scranton Road, San Diego, California 92121

Received: March 24, 1999; In Final Form: June 16, 1999

A set of nonbonded force field parameters consisting of atomic partial charges and van der Waals parameters has been derived by fitting experimental data for a broad set of organic compounds. The compounds in the fit spanned 11 functional groups: alcohols, aldehydes, amides, amines, carboxylic acids, esters, ethers, *N*-heterocycles, hydrocarbons, ketones, and sulfur compounds. The data consist of 136 crystal structures, 34 sublimation energies, and 63 gas-phase dipole moments. The nonbonded potential function is of the "9-6" form and is used in our class II CFF force field. This paper describes the fitting procedure and the quality of the fit as measured by comparing computed and experimental gas-phase dipole moments and crystal lattice energies. As a further test, each crystal structure was optimized. We report the accuracy of the computed crystal structures, including results obtained with force fields derived using two different combination rules. A summary is presented of the accuracy and consistency of predicted crystal lattice vectors and the lattice energies at the computed crystal structures. The results are discussed separately for each of the functional groups.

Introduction

During the past decade a great deal of effort has been devoted to the development of molecular mechanics and dynamics methods for simulating the properties of complex molecular systems. The applicability of all such simulations, however, is strongly dependent on the accuracy of the computational models employed. Key to the accuracy of virtually all atomistic molecular simulations is the potential energy function, or force field, which specifies the energy of the system as a function of atomic positions. The need for the development of accurate, transferable potential energy functions that meet the demands for both increased accuracy and broad applicability therefore remains high.

The derivation and testing of a next generation force field, focusing primarily on the valence (bonded) terms in the energy expression, have been the subject of previous papers in this series.[1−6] In this paper, we focus on the nonbonded interactions for organic functional groups. We examine the problems both of determining potential parameters from experimental data and of evaluating alternative functional forms for the potential. We have chosen as our source of data the crystal structures and lattice energies of crystals of representative organic compounds. Gas-phase dipole moments of a similar set of compounds were also used.

Nonbonded potentials may be determined in several ways, such as by fits to properties of neat liquids[7−9] or, more recently, directly from quantum mechanical calculations.[10,11] However, crystallographic data have been used to derive and test nonbonded components of force fields for many years[12−19] and continue to provide a number of advantages over other approaches. First, there is a large amount of highly precise data available, particularly from X-ray crystallography. Second, the different packing arrangements of various molecules with the same functional groups provide a range of intermolecular separations and orientations sampled by the experimental measurements. This leads to a larger experimental data set with which to derive well-determined nonbonded parameters. Finally, many of the properties we wish to simulate such as ligand−protein interactions and biomolecular structural properties correspond to "condensed-phase" ordered organic systems.

Hydrocarbons were among the first organic compounds whose crystal structures were used for determining nonbonded parameters.[12] Later, the availability of accurate crystal data, particularly sublimation energies and unit cell lengths and angles, as well as gas-phase data such as dipole moments, allowed the parametrization of species such as amides and carboxylic acids.[14−18,20,21] These parameters enabled the molecular modeling of several types of compounds of practical interest, especially peptides and proteins.[22] Crystal data were used in developing the CVFF force field[22] and versions of the AMBER[23−25] and CHARMM[26−29] force fields.

In this paper, we report the derivation of nonbonded parameters, van der Waals coefficients, and atomic partial charges, spanning a broad range of organic functional groups. Since a disparate set of functional groups is contained in the molecules we have studied, sampling a variety of molecular environments, key questions are the following. What levels of accuracy and precision may be obtained using the derived parameters in computing crystal properties using these techniques? Is the same method of deriving nonbonded parameters appropriate to all cases; i.e., are the resulting parameters of comparable accuracy for the differing species?

To examine the quality of the fit to the experimental data, we report the accuracy of the computed molecular dipole moments and the crystal lattice energies calculated using the experimental structures. In addition, crystal structure optimizations were performed and used to determine the deviations

† Alanex Corporation, 3550 General Atomics Court, San Diego, CA 92121.

‡ ScienceMedia Inc., 6540 Lusk Blvd., Suite C144, San Diego, CA 92121.

10.1021/jp991011l CCC: $18.00
Published on Web 08/03/1999

between the computed and experimental crystal lattice energies and unit cell parameters for each of the different functional groups.

The organization of the remainder of this paper is as follows. We first review the methodology for deriving all the terms in the nonbonded potential by fitting experimental crystal properties. These terms include both the Coulombic and van der Waals interactions. Crystal lattice vectors for a set of 136 crystals and lattice energies for 34 crystals, spanning 11 common organic functional groups, were used to derive the parameters. Gas-phase dipole moment data for each of the functional groups were also included in the fitting procedure. The resulting van der Waals parameters and atomic partial charges have been used in deriving the intramolecular terms in the current CFF force field (the nonbonded interactions being combined with torsional energies in computing vicinal 1−4 interactions).[1−6,30−33] The computed crystal properties are used to compare results with different combination rules for forming the nonbonded potential. The accuracies of the computed dipole moments (using our derived atomic partial charges) of the gas-phase compounds used in the fit are also described. We then present the results of test calculations in which the structure of each crystal used in the fit was optimized to compute its crystal structure and lattice energy using our derived nonbonded parameters. Finally, we discuss the accuracies of the computed crystal properties for each of the functional groups and summarize our results regarding the relative accuracies for the various types of compounds.

Methodology

1. Form of the Energy Function. The usual approximation to the nonbonded potential energy functions of molecules and molecular complexes is to express the energy as the sum of energies between pairs of atoms i and j, using functions of their position vectors $\vec{r}_i$ and $\vec{r}_j$,

$$E_{\text{nonbond}} = \sum_{i<j}^{\text{atoms}} E(\vec{r}_i - \vec{r}_j) = \sum_{i<j}^{\text{atoms}} E(r_{ij}) = \sum_{i<j}^{\text{atoms}} E_{\text{vdW}}(r_{ij}) + 332.071 \sum_{i<j}^{\text{atoms}} \frac{q_i q_j}{r_{ij}} \quad (1)$$

where r_{ij} is an interatomic distance, E_{vdW} is the corresponding van der Waals energy, and the last term is the sum of Coulombic interaction energies (in kcal/mol) between atomic partial charges q_i and q_j when charges are given in units of electrons and distances in angstroms. The summation is over all pairs of atoms i and j, where atoms i and j are in different molecules or are separated by at least three bonds within the same molecule. It is useful to express the q_i in terms of bond increments, δ_{ij}, which are the incremental partial charges contributed to atom i by all other atoms to which it is bonded,

$$q_i = q_{io} + \sum_j \delta_{ij} \quad (2)$$

where q_{io} is a formal charge. This has the advantage that the charge on each atom takes into account the nature of the other atoms to which it is bonded. For example, the partial charge on the nitrogen atom of primary amines may be different from that in secondary amines, even though the nitrogen may be assigned the same force field atom type in both species. q_{io} is set to zero except for formally charged groups, such as ammonium or carboxylate. Here, we use the convention of defining δ_{ij} such that positive δ_{ij} corresponds to positive charge being donated from atom j to atom i. In addition, the δ_{ij} are constrained such that $\delta_{ji} = -\delta_{ij}$. Thus, parametrizing the atomic partial charges using bond increments has the additional advantage that

$$\sum_i^{\text{atoms}} q_i = \sum_i^{\text{atoms}} q_{io} \qquad (=0 \text{ except for ions}) \quad (3)$$

so that, for example, for uncharged molecules the sum of the partial charges derived from bond increments will always be zero.

The van der Waals energy, $E_{\text{vdW}}(r_{ij})$, can be written as

$$E_{\text{vdW}}(r_{ij}) = \epsilon_{ij}\left[\left(\frac{m}{n-m}\right)\left(\frac{r^*_{ij}}{r_{ij}}\right)^n - \left(\frac{n}{n-m}\right)\left(\frac{r^*_{ij}}{r_{ij}}\right)^m\right] \quad (4)$$

where m and n are integers and r^*_{ij} and ϵ_{ij} are the van der Waals radius and well depth parameters, respectively. Often, the van der Waals energy is chosen to be a "12-6" potential ($n = 12$, $m = 6$),

$$E_{\text{vdW}}(r_{ij}) = \epsilon_{ij}\left[\left(\frac{r^*_{ij}}{r_{ij}}\right)^{12} - 2\left(\frac{r^*_{ij}}{r_{ij}}\right)^6\right] \quad (5)$$

or, equivalently,

$$E_{\text{vdW}}(r_{ij}) = \left[\left(\frac{A_{ij}}{r_{ij}^{12}}\right) - \left(\frac{B_{ij}}{r_{ij}^{6}}\right)\right] \quad (6)$$

where

$$r^*_{ij} = \left(\frac{2A_{ij}}{B_{ij}}\right)^{1/6} \quad (7)$$

$$\epsilon_{ij} = \left(\frac{B_{ij}^2}{4A_{ij}}\right) \quad (8)$$

and

$$A_{ij} = \epsilon_{ij}(r^*_{ij})^{12} \quad (9)$$

$$B_{ij} = 2\epsilon_{ij}(r^*_{ij})^6 \quad (10)$$

Similarly, for a "9-6" potential ($n = 9$, $m = 6$),

$$E_{\text{vdW}}(r_{ij}) = \epsilon_{ij}\left[2\left(\frac{r^*_{ij}}{r_{ij}}\right)^9 - 3\left(\frac{r^*_{ij}}{r_{ij}}\right)^6\right] \quad (11)$$

If interacting atom types i and j are not the same, combination rules are generally used to approximate ϵ_{ij} from the values of ϵ_i and ϵ_j as well as r^*_{ij} from r^*_i and r^*_j. One widely used approach is to form the arithmetic and geometric means,

$$r^*_{ij} = (r^*_i + r^*_j)/2 \quad (12)$$

$$\epsilon_{ij} = (\epsilon_i \epsilon_j)^{1/2} \quad (13)$$

However, it has been shown that other combination rules, such as the ones proposed by Waldman and Hagler (WH),[34] generally give better accuracy. The WH combination rules are

$$r^*_{ij} = \left(\frac{r^{*6}_i + r^{*6}_j}{2}\right)^{1/6} \quad (14)$$

$$\epsilon_{ij} = 2(\epsilon_i \epsilon_j)^{1/2} \left(\frac{r^*_i{}^3 r^*_j{}^3}{r^*_i{}^6 + r^*_j{}^6} \right) \quad (15)$$

Except where noted, WH combination rules were used in determining all the van der Waals parameters and computed crystal properties reported herein.

2. Observables Used in Parametrization. *Sublimation Energies.* The first type of experimental crystal data used to derive the nonbonded parameters is the sublimation energy, which is the amount of energy required to transfer a molecule from the crystal to the gas phase,

$$\Delta H_s = \Delta H_{gas} - \Delta H_{lat}$$

where ΔH_{gas} and ΔH_{lat} are the enthalpies of formation of the gas and crystal lattice, respectively. In the ideal gas approximation, this may be approximated as[15]

$$\Delta H_s = (E_{gas}^{intra} + E_{gas}^{vib} + 4RT) - (E_{lat}^{intra} + E_{lat}^{inter} + E_{lat}^{intravib} + E_{lat}^{intervib}) \quad (16)$$

where $4RT$ is the pressure−volume term plus rotational energy in the gas phase, and the gas-phase energies E_{gas}^{intra} and E_{gas}^{vib} are the intramolecular potential energy and the vibrational energy, respectively. The lattice energies E_{lat}^{intra} and E_{lat}^{inter} are the intramolecular and intermolecular potential energies, and $E_{lat}^{intravib}$ and $E_{lat}^{intervib}$ are the intramolecular and intermolecular vibrational energies in the crystal, respectively. If the additional approximations are made such that (1) the intramolecular potential energy is the same in the gas and the solid phases, (2) the intramolecular vibrational energies are also the same in the gas and the crystal, and (3) $E_{lat}^{intervib}$ is approximately $6RT$ from the Debye−Einstein model,[35] eq 16 simplifies to[15,35]

$$\Delta H_s = -2RT - E_{lat}^{inter} \quad (17)$$

where E_{lat}^{inter} is the lattice energy, which will be referred to below as simply E_{lat}.

If $\vec{a}_1$, $\vec{a}_2$, and $\vec{a}_3$ are the three lattice vectors specifying the edges of the unit cell, the translation vector to the origin of the coordinate system of the kth neighboring unit cell, $\vec{b}_k$, is uniquely specified by three integers l_{k1}, l_{k2}, and l_{k3},

$$\vec{b}_k = \sum_{m=1}^{3} l_{km} \vec{a}_m \quad (18)$$

The lattice energy is then related to the pairwise interatomic nonbond energy E_{ij} by the expression

$$E_{lat} = \frac{1}{2} \sum_{i}^{atoms} \sum_{j}^{atoms} E_{ij}(|\vec{r}_i - \vec{r}_j|) + \frac{1}{2} \sum_{i}^{atoms} \sum_{j}^{atoms} \sum_{k}^{cells} E_{ij}(|\vec{r}_i - (\vec{r}_j + \vec{b}_k)|) \quad (19)$$

where the summations over i include all atoms of the molecules in the unit cell. In the first sum, j includes the atoms of all molecules in the central unit cell other than the molecule containing atom i. In the second sum, j includes the atoms of all molecules in the central unit cell, and k extends over all cells in the crystal surrounding the central unit cell. Thus, knowing the experimental lattice vectors $\vec{a}_1$, $\vec{a}_2$, and $\vec{a}_3$ allows the experimental ΔH_s to be related to the nonbonded interaction energies $E(r_{ij})$ using eqs 17 and 19. In our procedure E_{lat} is computed at the experimental crystal geometry, and the sum of squared differences over all crystal structures between the values of E_{lat} given by eqs 17 and 19 is minimized in fitting the nonbonded parameters.

Crystal Lattice Vectors. It is generally not necessary to fit the crystal lattice vectors directly using the nonbonded potential function, which would require computing the equilibrium structure of each crystal at each step of the fitting process. It is possible to use the fact that at equilibrium the derivative of the lattice energy of each crystal with respect to each of the components of its lattice vectors is zero. If a lattice vector component for a given crystal is denoted as a_i, the computed derivative of the lattice energy at the calculated equilibrium structure may be written as a Taylor series,

$$\left.\frac{\partial E_{lat}}{\partial a_i}\right|_{calc} = \left.\frac{\partial E_{lat}}{\partial a_i}\right|_{expt} + \left.\frac{\partial^2 E_{lat}}{\partial a_i{}^2}\right|_{expt} \Delta a_i + \ldots \quad (20)$$

where Δa_i is the difference between the experimental and calculated lattice vector component, and the quantities on the right-hand side of eq 20 are evaluated at the experimental crystal structure. At the calculated minimum energy structure the derivative is zero. When the left-hand side of this equation is set to zero and when higher order terms are neglected, the difference between the calculated and experimental lattice vector component may be approximated as

$$\Delta a_i = -\left(\left.\frac{\partial^2 E_{lat}}{\partial a_i{}^2}\right|_{expt} \right)^{-1} \left.\frac{\partial E_{lat}}{\partial a_i}\right|_{expt} \quad (21)$$

Since the goal is to determine the parameters that yield the experimental structure as the minimum, the magnitude of the Δa_i is minimized with respect to the nonbonded parameters.

Gas-Phase Dipoles. The magnitudes of the gas-phase dipole moment vectors were also used in fitting the atomic partial charges as parametrized by the bond increments. At the experimental geometry, the dipole moment $\vec{\mu}$ is given by

$$\vec{\mu} = \sum_{i}^{atoms} q_i \vec{r}_i = \sum_{i}^{atoms} \vec{r}_i \sum_{j}^{bonded\ atoms} \delta_{ij} \quad (22)$$

where $\vec{r}_i$ is the distance vector from the origin of the molecular coordinate system, the index i is summed over all atoms, and j is summed over all other atoms directly bonded to i. The magnitudes of the computed dipole moments, $|\vec{\mu}|$, are then fit to the experimental dipole moments by adjusting the bond increments δ_{ij}.

3. Fitting Procedure. All the experimental data were fit simultaneously to obtain the van der Waals parameters and bond increments. The objective function S was the weighted sum of the squared deviations between the computed and experimental lattice vector components Δa_i, dipole moments $\Delta\vec{\mu}$, and lattice energies ΔE_{lat} so that

$$S = w_{lat} \sum_{i}^{crystals} (\Delta E_{lat_i})^2 + w_\mu \sum_{i}^{molecules} (\Delta\mu_i)^2 + w_a \sum_{i}^{crystals} \sum_{j}^{vectors} |\Delta a_{ij}|^2 \quad (23)$$

where the index i specifies the crystals in the first and third sums, the molecules in the second, and j the crystal lattice vectors in the third. The weighting factors w_{lat}, w_μ, and w_a were adjusted to ensure that these observed quantities all had

approximately the same relative deviations. This resulted in the values $w_\mu = w_a = 10$, $w_{lat} = 1$.

In the calculation of the lattice energies and their derivatives, a lattice segment of five unit cells per side was constructed around the central unit cell. A molecular cutoff radius (maximum internuclear distance) of 15 Å was then used. The cutoff was applied such that if the distance between atoms in any two molecules was less than the cutoff radius, then the entire intermolecular energy between the two molecules was included in the calculation. Thus, the effective cutoff distance for the interatomic interactions was significantly greater than 15 Å. In some crystals, the experimental coordinates included only the nonhydrogen atoms. In these cases the hydrogen atoms were constructed by optimizing their bond lengths and angles using the CVFF force field. The parameter optimization based on eq 23 was then carried out using MSI's Vibgeom and Crystal programs employing a quasi-Newton minimization algorithm.[36]

4. Validation Method. To assess the accuracy of the force field, the structure of each crystal used in fitting the nonbonded parameters was optimized by minimizing its lattice energy using the final derived parameters. The minimum energy configuration was determined by fixing one molecule in the unit cell and varying the relative positions and orientations of all other molecules in the unit cell starting with the experimental crystal structure. The unit cell vectors were also varied. Thus, minimization of a crystal having Z molecules per unit cell involves $6(Z - 1) + 9$ degrees of freedom: six degrees for the rigid body rotation and translation of all but one molecule in the unit cell, and nine degrees for the Cartesian representations of the unit cell vectors. This method contrasts with other procedures that vary only those degrees of freedom allowed by crystal symmetry. The present less constrained minimization is a more stringent test of the potential because crystal symmetry is now derived rather than imposed.

As in the lattice energy calculations used in deriving the nonbonded parameters, energy minimizations were carried out by considering a lattice segment of five unit cells related by translational symmetry in each direction and with a molecular cutoff radius of 15 Å. The lattice energy for the central unit was minimized with a quasi-Newton algorithm until the forces with respect to the lattice vector components, the rigid body translations, and rigid body rotations were each below 10^{-5} kcal mol^{-1} Å^{-1} or 10^{-5} kcal mol^{-1} rad^{-1}.

Results

1. Parameter Fitting. To derive the nonbonded parameters with a reasonable number of adjustable parameters, it is useful first to assign atom types to each atom in each molecule. The 16 atom types we have used in this study are listed in Table 1. These are the same types employed for this subset of molecules by the CFF force field.[1-6] The optimized van der Waals parameters, r^* and ϵ, for each atom type are given in Table 2. These parameters were derived using the Waldman−Hagler (WH) combination rules as defined by eqs 14 and 15. Table 3 gives the bond increments between atom types for all bonds that occur in the parametrized set of molecules.

Experimental data for 179 compounds were used in deriving the parameters. The structures of the compounds are given in Figure 1. The data consisted of 136 crystal structures, 34 sublimation energies, and 63 gas-phase dipole moments. The crystal structures are from X-ray and neutron diffraction measurements. They correspond to a range of temperatures, but most were chosen to be well below room temperature and were typically measured in the range 50−150 K. Most of the gas-

TABLE 1: Types Assigned to Atoms in Various Functional Groups in the CFF Force Field

atom type	molecular connectivity
c	carbon (sp^3) in alkanes
c″	carbonyl carbon in aldehydes, carboxylic acids, esters, and ketones
c′	carbonyl carbon in amides (connected to nitrogen)
c=	carbon (sp^2) in alkenes
cp	carbon in aromatic rings
ct	carbon (sp) in alkynes
h	hydrogen connected to carbon
h*	hydrogen connected to oxygen or nitrogen
n	nitrogen in amides
na	nitrogen (sp^3) in amines
nh	nitrogen (sp^2) triply connected in five- and six-membered rings (e.g., pyrrole)
nn	nitrogen (sp^2) connected to aromatic rings (e.g., aniline)
np	nitrogen (sp^2) doubly connected in five- and six-membered rings (e.g., pyridine)
o	doubly connected oxygen
o′	carbonyl oxygen
s	sulfur (sp^3) doubly connected

TABLE 2: van der Waals Parameters Derived by Fitting the Crystal Data with the 9-6 Potential and Waldman−Hagler Combination Rules

atom type	r^* (Å)	ϵ (kcal/mol)
c	4.010	0.054
c′, c″	3.308	0.120
c=, cp, ct	4.010	0.064
h	2.995	0.020
h*	1.098	0.013
n	4.070	0.106
na	4.070	0.065
nh, nn, np	3.700	0.170
o	3.535	0.240
o′	3.535	0.267
s	4.027	0.071

TABLE 3: Bond Increments Obtained by Simultaneously Fitting the Crystal and Gas-Phase Data[a]

atom types		bond increment
i	j	δ_{ij}
c	h	−0.0530
c	n	0.2108
c	na	0.0827
c	nh	0.2108
c	o	0.1133
c	s	0.0650
c′	cp	0.0650
c′	h	−0.0456
c′	nh	0.0700
c′	o′	0.3964
c″	o	0.0030
c″	cp	0.0650
c″	h	−0.0456
c″	o′	0.3964
c=	h	−0.1268
c=	s	−0.0120
cp	h	−0.1400
cp	nh	0.1600
cp	nn	0.0400
cp	np	0.1800
cp	o	0.1500
cp	s	−0.0120
h*	n	0.4395
h*	na	0.2487
h*	nh, nn	0.3700
h*	o	0.4241

[a] A positive value means positive charge is donated to the first atom from the second. Units are electronic charge. Except where listed, δ_{ij} is set to zero for all bonds between atoms of the same chemical element.

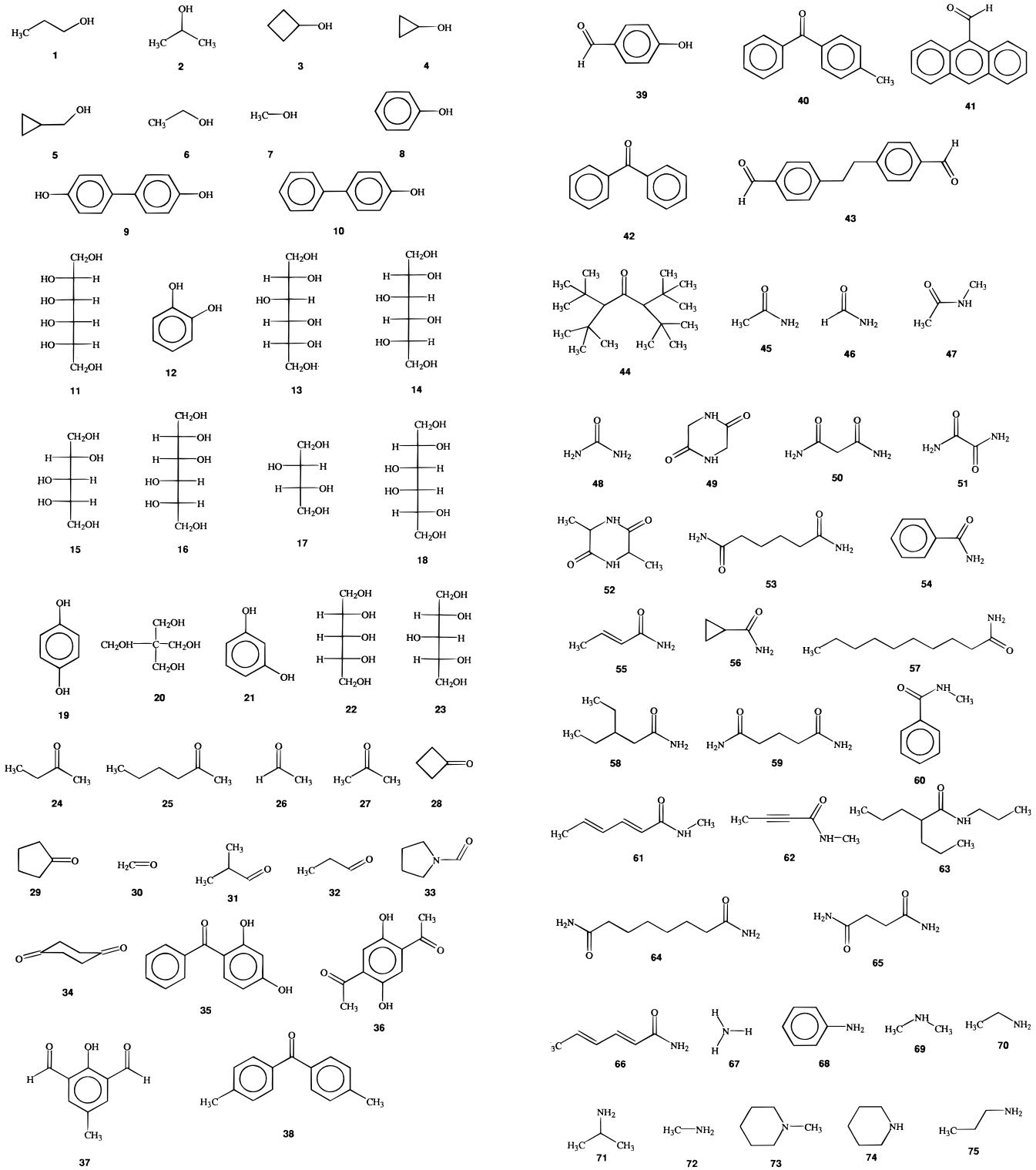

Figure 1. Molecular structures of the compounds whose experimental data were employed in fitting the nonbonded parameters. Structures **1**−**23** comprise the alcohols, **24**−**44** the aldehydes and ketones, **45**−**66** the amides, **67**−**86** the amines, **87**−**105** the carboxylic acids, **106**−**114** the esters, **115**−**124** the ethers, **125**−**134** the nitrogen heterocycles, **135**−**160** the hydrocarbons, and **161**−**179** the sulfur compounds.

phase data were taken from the compilation by Nelson, Lide, and Maryott[37] and references therein. These authors recommend "best" values of the dipole moments based on evaluation of several measurements and differing types of experimental techniques. The remainder of the dipole moment data was taken from reported microwave measurements (see references in Table 4).

We use the same nomenclature for the names of the compounds as used by the authors of the experimental papers we cite except for cases where the authors' nomenclature is either unusual or the nomenclature varies in different reports. To help identify the compounds, we list the Chemical Abstracts Service registry number of each compound employed. A list of all the compounds used in fitting the crystal structures along with the number corresponding to each molecular structure as shown in Figure 1, its CAS registry number, and the reference to the experimental data is given in Table 10. The compounds whose gas-phase data were employed, the structure number

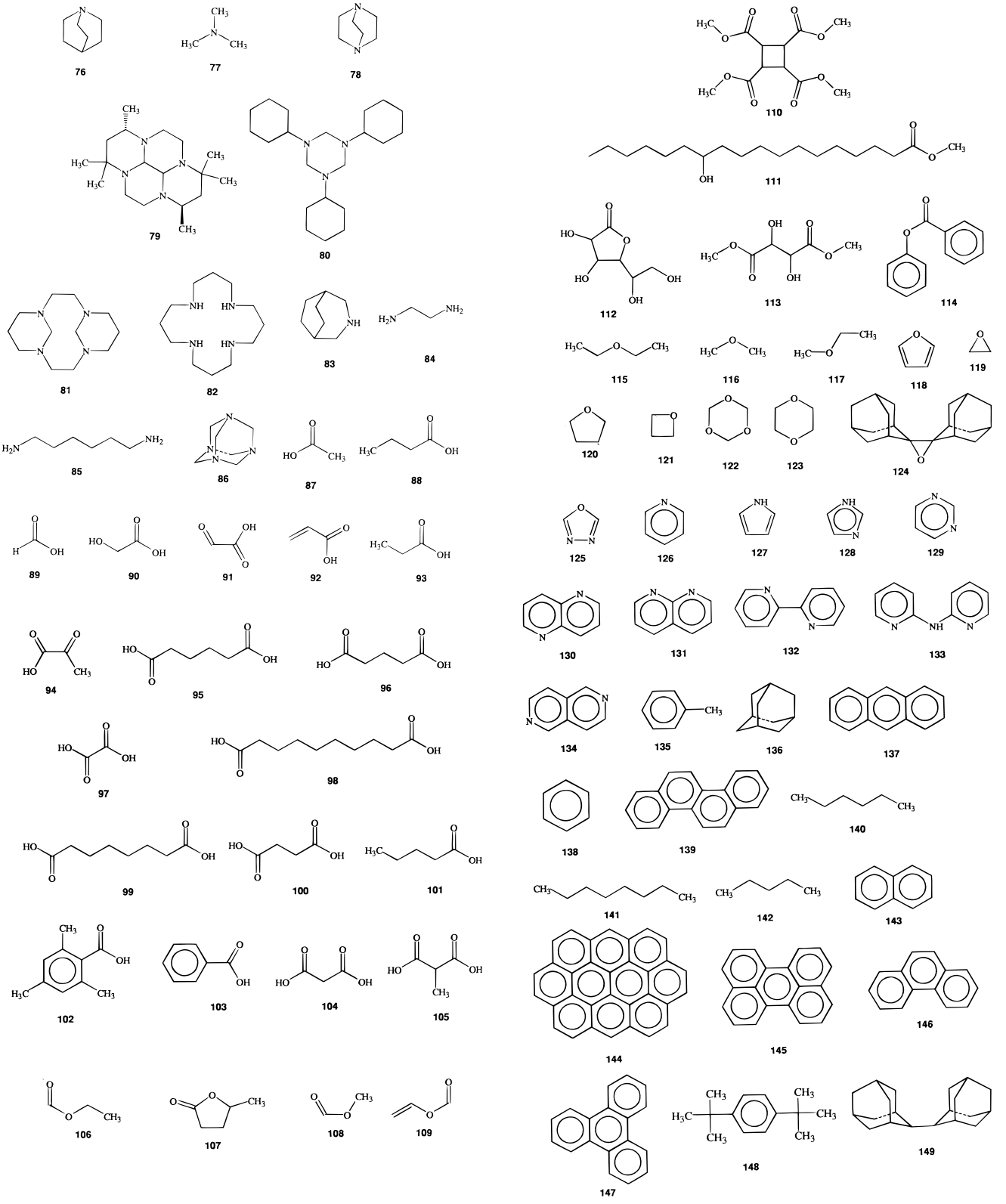

Figure 1. Continued.

(Figure 1), its registry number, its experimental dipole moment, and the reference to the experimental measurement, are given in Table 4. A similar compilation is given in Table 5 for the lattice energies.

The data for the hydrocarbons were fit first, since alkyl moieties occur in nearly all of the compounds. The nonbonded parameters for the carbon and hydrogen were then transferred in fitting the data for the other species.

2. Summary of Test Calculations. *Effect of Combination Rule on Optimized Parameters.* In Table 6 we compare the effect of using different combination rules (in this case the arithmetic−geometric mean (AG) (eqs 12 and 13) and Waldman−Hagler (WH) rules (eqs 14 and 15) on the values of the optimized r^* and ϵ parameters for a subset of atom types. Both sets of parameters are based on the "9-6" form of the potential. Atomic partial charges and van der Waals parameters were derived in

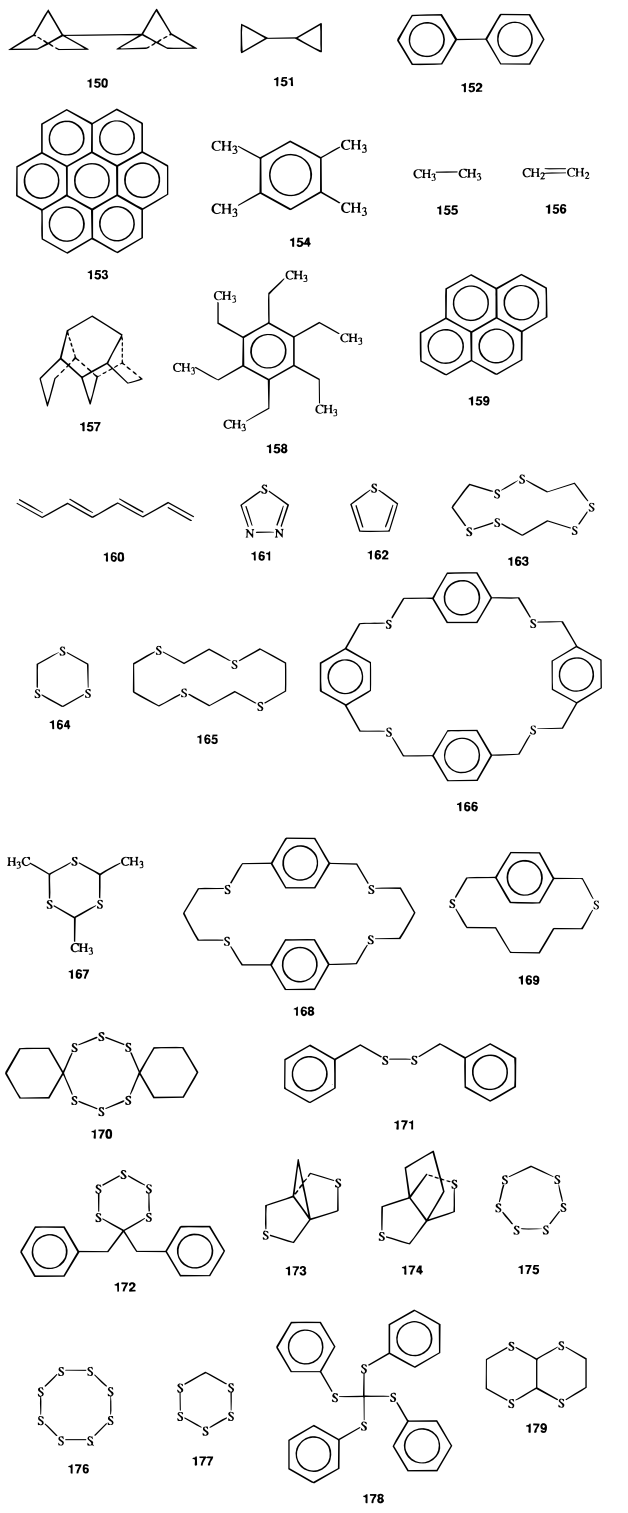

Figure 1. Continued.

precisely the same way for the two combination rules (described above). The differences in r^* are moderate, the AG rules almost always giving the larger values. The greatest difference arises for the np (doubly connected ring nitrogen) atom type, for which the WH rules give 3.57 Å while the AG rules give 4.30 Å. For ϵ values there is no systematic difference between the two combination rules, although the percentage differences tend to be much larger than for r^*. Thus, for o′ (carbonyl oxygen) the WH value of 0.267 kcal/mol is over 7 times larger than the AG value of 0.038 kcal/mol. The accuracy of calculated properties obtained with the two combination rules is described below.

Effect of Differing Combination Rules on Computed Crystal Structures. To assess the accuracies of the crystal simulations using our derived parameters, we first examined the results of using the WH combination rules compared to the standard AG combination rules. The structures for a subset of 93 crystals comprising seven families were computed using the nonbonded parameters given in Table 6. The resulting deviations in the crystal structures are given in Table 7. This includes the rms deviations between experimental and calculated values for unit cell lengths, unit cell angles, and the intermolecular distances between heavy atoms separated by less than 4 Å. The results indicate a (perhaps surprising) significant dependence on combination rule. They indicate (Table 7) that the use of the WH rules gives more accurate results (smaller rms deviations) for the crystal properties studied. The AG rules give about the same or marginally more accurate results only for the amides and amines. For alcohols, the deviations with the AG rules are roughly twice those obtained with the WH rules.

Overall Accuracy of CFF. The experimental and computed gas-phase dipole moments for each of the molecules included in the fit were given in Table 4. In Table 8 we collect the rms deviations in dipole moments for each of the functional groups (excluding hydrocarbons). The deviation is lowest for the amides (0.12 D) and greatest for the aldehydes and ketones (0.46 D).

To further test the complete set of derived nonbonded parameters, the energy of each crystal was minimized with respect to all the degrees of freedom, i.e., position and orientation of the molecules in the unit cell as well as the lattice vectors. The accuracy achieved as reflected in the unit cell lengths, angles, lattice energies, and interatomic distances between molecules are summarized in Table 9 for each of the families. Since the number of experimental enthalpies of sublimation is substantially less than the number of crystal structures, the number of lattice energies for each family used is given in parentheses. There are consistently a few hundred interatomic distances less than 4 Å between molecules per unit cell for each functional group.

The calculated relative lattice energies of different molecules in a family obey expected trends, such as the increase with increasing number of polar functional groups. For example, in the series *n*-pentane, valeric acid, and glutaric acid (i.e., $CH_3-(CH_2)_3-CH_3$, $CH_3-(CH_2)_3-COOH$, and $HOOC-(CH_2)_3-COOH$) adding carboxylate groups increases the computed lattice energy from −9.8 to −20.1 and −31.6 kcal/mol, respectively, in good agreement with the experimental values[17,35] of −11.1, −20.2, and −29.0 kcal/mol, respectively. Similarly increasing the chain length in dibasic acids on going from succinic ($HOOC-(CH_2)_2-COOH$) to sebacic acid ($HOOC-(CH_2)_7-COOH$) increases the lattice energy from −31.4 to −41.0 kcal/mol, in agreement with the experimental values,[38,39] which increase from −29.3 to −39.6 kcal/mol.

Comparison of a range of crystal properties is necessary in order to fully gauge the accuracy of the force field. In particular, deviations in the unit cell lengths are not always reliable indicators of the differences between the calculated and experimental crystal structures because they reflect cumulative deviations in intermolecular distances along lattice vectors, which depend on the number of molecules in the unit cell and the particular packing structure of the crystal. For example, if eight molecules are stacked along a unit cell vector, then a 0.10 Å deviation in the distance between a pair of molecules will lead to a 0.80 Å deviation in the unit cell length.

Considering the range of molecular sizes, topologies, types of crystal packing and charge distributions represented by the molecular families in Table 9, it is comforting that the rms

TABLE 4: Experimental and Calculated Values of Gas-Phase Dipole Moments[a]

molecule	molecule no.	registry no.	ref	dipole moment (D) exptl	dipole moment (D) computed	dipole moment (D) deviation
		Alcohols				
1-propanol	1	71-23-8	37	1.68	1.93	(−0.25)
2-propanol (*t*)	2	67-63-0	59	1.58	1.86	(−0.28)
cyclobutanol	3	2919-23-5	60	1.62	1.61	(0.01)
cyclopropanol (*g*)	4	16545-68-9	40	1.46	1.89	(−0.43)
cyclopropylcarbinol	5	2516-33-8	61	1.87	1.72	(0.15)
ethanol	6	64-17-5	37	1.69	1.96	(−0.27)
methanol	7	67-56-1	37	1.70	1.91	(−0.21)
phenol	8	108-95-2	37	1.45	1.12	(0.33)
		Aldehydes and Ketones				
2-butanone (*t*)	24	78-93-3	62	2.78	2.62	(0.16)
2-hexanone	25	591-78-6	63	2.66	2.64	(002)
acetaldehyde	26	75-07-0	37	2.69	2.46	(0.23)
acetone	27	67-64-1	37	2.88	2.59	(0.29)
cyclobutanone	28	1191-95-3	64	2.89	2.52	(0.37)
cyclopentanone	29	120-92-3	65	3.25	2.61	(0.64)
formaldehyde	30	50-0-0	37	2.33	2.29	(0.04)
isobutanal (*c*)	31	78-84-2	66	2.69	2.45	(0.24)
isobutanal (*t*)	31	78-84-2	66	2.89	2.44	(0.45)
propanal (*c*)	32	123-38-6	37	2.52	2.50	(0.02)
pyrrolidine carboxaldehyde	33	3760-54-1	41	4.47	3.40	(1.07)
		Amides				
acetamide	45	60-35-5	67	3.68	3.86	(−0.18)
formamide	46	75-12-7	15	3.73	3.85	(−0.12)
N-methylacetamide	47	79-16-3	15	3.73	3.80	(−0.07)
urea	48	57-13-6	15	4.45	4.53	(−0.08)
		Amines				
ammonia	67	7664-41-7	37	1.47	1.36	(0.11)
aniline	68	62-53-3	37	1.53	1.52	(0.01)
dimethylamine	69	124-40-3	37	1.03	0.92	(0.11)
ethylamine (*g*)	70	75-04-7	37	1.22	1.21	(0.01)
ethylamine (*t*)	70	75-04-7	68	1.30	1.19	(0.11)
isopropylamine (*t*)	71	75-31-0	69	1.19	1.16	(0.03)
methylamine	72	74-89-5	37	1.31	1.16	(0.15)
N-methylpiperidine	73	626-67-5	70	0.75	0.78	(−0.03)
piperidine	74	110-89-4	70	1.15	1.02	(0.13)
propylamine	75	107-10-8	37	1.17	1.17	(0.00)
quinuclidine	76	100-76-5	45	1.20	0.88	(0.32)
trimethylamine	77	75-50-3	37	0.61	0.85	(−0.24)
		Carboxylic Acids				
acetic acid	87	64-19-7	17	1.74	1.67	(0.07)
butyric acid	88	107-92-6	17	1.68	1.89	(−0.21)
formic acid (*c*)	89	64-18-6	17	1.42	1.83	(−0.41)
formic acid (*t*)	89	64-18-6	17	3.79	4.16	(−0.37)
glycolic acid	90	79-14-1	50	2.16	2.77	(−0.61)
glyoxylic acid	91	298-12-4	71	1.86	1.92	(−0.06)
propenoic acid (*c*)	92	79-10-7	72	1.46	1.66	(−0.20)
propenoic acid (*t*)	92	79-10-7	72	2.02	1.64	(0.38)
propionic acid	93	79-09-4	17	1.76	1.70	(0.06)
pyruvic acid	94	127-17-3	73	2.30	1.99	(0.31)
		Esters				
ethyl formate (*g*)	106	109-94-4	74	1.81	1.87	(−0.06)
ethyl formate (*t*)	106	109-94-4	74	1.98	1.83	(0.15)
γ-valerolactone	107	108-29-2	53	4.71	4.48	(0.23)
methyl formate	108	107-31-3	37	1.77	1.88	(−0.11)
vinyl formate	109	692-45-5	37	1.48	1.70	(−0.22)
		Ethers				
diethyl ether	115	60-29-7	37	1.15	1.17	(−0.02)
dimethyl ether	116	115-10-6	37	1.30	1.17	(0.13)
ethylmethyl ether	117	540-67-0	37	1.23	1.16	(0.07)
furan	118	110-00-9	37	0.66	0.43	(0.23)
oxirane	119	75-21-8	37	1.89	1.52	(0.37)
tetrahydrofuran	120	109-99-9	37	1.63	1.17	(0.46)
trimethylene oxide	121	503-30-0	37	1.94	1.34	(0.60)
		N-Heterocycles				
1,3,4-oxadiazole	125	288-99-3	37	3.04	3.38	(−0.34)
pyridine	126	110-86-1	37	2.19	2.17	(0.02)
pyrrole	127	109-97-7	37	1.84	1.72	(0.12)
		Hydrocarbons				
toluene	135	108-88-3	37	0.36	0.36	(0.00)
		Sulfur Compounds				
1,3,4-thiadiazole	161	110-02-1	37	3.29	3.01	(0.28)
thiophene	162	288-47-1	37	0.55	0.82	(−0.27)

[a] When more than one conformer has been studied, the specific conformer is denoted by *c* for cis, *g* for gauche, or *t* for *trans.* Deviations (experimental minus computed values) are given in parentheses.

TABLE 5: Experimental and Calculated Crystal Lattice Energies[a]

crystal	molecule no.	registry no.	ref	energies (kcal/mol) exptl	computed	deviation
		Aldehydes and Ketones				
1,4-cyclohexanedione	34	637-88-7	42	21.3	19.7	(1.6)
		Amides				
diketopiperazine	49	106-57-0	75	26.0	28.5	(−2.5)
formamide	46	75-12-7	76	17.5	15.7	(1.8)
malonamide	50	108-13-4	15	28.8	28.9	(−0.1)
N-methylacetamide	47	79-16-3	77	18.0	17.1	(0.9)
oxamide	51	471-46-5	78	28.2	25.9	(2.3)
urea	48	57-13-6	79	22.2	22.2	(0.0)
		Amines				
triethylenediamine	78	280-57-9	38	14.8	14.5	(0.3)
		Carboxylic Acids				
acetic acid	87	64-19-7	17	16.3	16.1	(0.2)
adipic acid	95	124-04-9	38	32.1	34.9	(−2.8)
butyric acid	88	107-92-6	17	19.2	19.0	(0.2)
formic acid	89	64-18-6	17	15.2	14.7	(0.5)
glutaric acid	96	110-94-1	17	29.0	31.6	(−2.6)
oxalic acid, α	97	144-62-7	80	24.8	31.9	(−7.1)
oxalic acid, *β*	97	144-62-7	80	23.5	30.9	(−7.4)
propionic acid	93	79-09-4	17	17.7	17.5	(0.2)
sebacic acid	98	111-20-6	39	39.6	41.0	(−1.4)
suberic acid	99	505-48-6	39	35.4	36.8	(−1.4)
succinic acid	100	110-15-6	38	29.3	31.4	(−2.1)
valeric acid	101	109-52-4	17	20.2	20.1	(0.1)
		N-Heterocycles				
imidazole	128	288-32-4	42	20.5	20.7	(−0.2)
pyrimidine	129	289-95-2	54	13.1	12.1	(1.0)
		Hydrocarbons				
adamantane	136	281-23-2	81	15.2	17.0	(−1.8)
anthracene	137	120-12-7	82	26.2	24.5	(1.7)
benzene	138	71-43-2	82	11.8	11.3	(0.5)
chrysene	139	218-01-9	82	32.5	30.9	(1.6)
n-hexane	140	110-54-3	35	13.2	11.8	(1.4)
n-octane	141	111-65-9	35	17.3	15.6	(1.7)
n-pentane	142	109-66-0	35	11.1	9.8	(1.3)
naphthalene	143	91-20-3	82	18.6	17.9	(0.7)
ovalene	144	190-26-1	83	50.6	46.6	(4.0)
perylene	145	198-55-0	56	35.7	31.7	(4.0)
phenanthrene	146	85-01-8	82	23.3	23.3	(0.0)
triphenylene	147	217-59-4	82	31.4	28.7	(2.7)

[a] α and *β* denote polymorphic forms of the crystal structure. Deviations (experimental minus computed values) are given in parentheses.

TABLE 6: Comparison of van der Waals Parameters Obtained with Arithmetic−Geometric Mean Combination Rules (AG) and Waldman−Hagler Combination Rules (WH)

atom type	*r** (Å) WH	*r** (Å) AG	ϵ (kcal/mol) WH	ϵ (kcal/mol) AG
c	4.010	4.500	0.054	0.037
c′	3.308	3.530	0.120	0.249
c″	3.308	3.530	0.120	0.249
cp	4.010	4.200	0.064	0.057
h	2.995	2.964	0.020	0.017
h*	1.098	1.098	0.013	0.013
n	4.070	4.275	0.106	0.224
na	4.070	4.100	0.065	0.062
nh	4.070	4.300	0.134	0.470
np	3.570	4.300	0.410	0.470
o	3.535	4.000	0.240	0.045
o′	3.535	3.691	0.267	0.038
s	4.027	4.900	0.071	0.020

deviations between the computed and experimental properties exhibit such consistent behavior. However, unusually large or small deviations in some properties are found for certain classes of molecules. In the following section we discuss each individual class of molecule, noting these deviations as appropriate. The numbering of the molecules corresponds to that used in Figure 1.

3. Results for Specific Classes of Molecules. *Alcohols.* The alcohols whose dipole moments were used in deriving the atomic partial charges included seven aliphatic (**1**−**7**) and one aromatic compound (phenol, **8**), as given in Table 4. The rms deviation in dipole moments between calculated and experimental values is 0.26 D, the deviation being largest for cyclopropanol (**4**, computed 1.89 D versus experimental[40] 1.46 D). No crystal sublimation energies of alcohols were employed in the parametrization. The lattice vectors of the crystals of 16 alcohols were included in the fit, including aliphatic compounds ranging from one hydroxyl group (ethanol, **6**) to six hydroxyls (allitol, **11**), aromatic compounds with one phenyl ring (catechol, *γ*-hydroquinone, and resorcinol **12**, **19**, and **21**), and two biphenyl derivatives (4,4′-dihydroxy- and 4-hydroxybiphenyl, **9** and **10**). The crystal structures all exhibit intermolecular hydrogen bonding, with the hydroxyl hydrogen atoms pointing toward an oxygen in a neighboring molecule (**I**). In the crystals the O−H bond is found to be either gauche or trans to the adjacent C−C or C−H bonds.

As shown in Table 9, the deviations in the unit cell lengths and angles are 0.21 Å and 1.63°, respectively, while the rms deviation in the nonbonded interatomic distances less than 4 Å is 0.12 Å. Altogether, 4971 such distances were used for an

TABLE 7: Effect of Differing Combination Rules on Computed Crystal Structures: Root-Mean-Square Deviations from Experimental Unit Cell Lengths, Angles, and Interatomic Distances between Molecules Less Than 4 Å with Waldman−Hagler Combination Rules (WH) and with Arithmetic−Geometric Mean Combination Rules (AG)

		rms deviation					
		unit cell length (Å)		unit cell angle (deg)		distance of <4 Å (Å)	
molecule type	no. of crystals	WH	AG	WH	AG	WH	AG
alcohols	12	0.13	0.33	1.91	3.45	0.09	0.17
amides	12	0.26	0.24	1.78	1.74	0.15	0.16
amines	9	0.16	0.15	1.09	0.80	0.14	0.13
carboxylic acids	14	0.35	0.62	3.20	4.34	0.20	0.36
N-heterocycles	9	0.41	0.39	1.49	2.46	0.17	0.21
hydrocarbons	22	0.11	0.16	1.64	2.73	0.21	0.27
sulfur compds	15	0.35	0.91	2.50	2.83	0.18	0.47
total/average rms	93	0.25	0.40	1.94	2.62	0.16	0.25

TABLE 8: Root-Mean-Square Deviations (in debye) between Experimental and Fitted Dipole Moments

molecule type	no. of molecules	rms deviation
alcohols	8	0.26
aldehydes & ketones	11	0.46
amides	4	0.12
amines	12	0.14
carboxylic acids	10	0.32
esters	5	0.17
ethers	7	0.33
N-heterocycles	3	0.21
sulfur compounds	2	0.27

average of 311 per crystal. A more detailed analysis reveals that the rms deviation in both O···H and O···O hydrogen bond

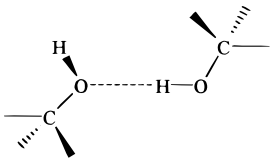

I

distances is 0.05 Å and in OH···O angles 2.23° over 53 such hydrogen bonds examined, with the computed O···H distances being slightly shorter than the experimental values for 80% of the distances examined. Since the rms deviation in all nonbonded distances is 0.12 Å, the hydrogen bond distances are more accurately computed than the other types of nonbonded distances. In each case the crystal symmetry was reproduced by the optimization. In general, the saturated alcohols are more accurately modeled than the aromatic alcohols. For example, 4,4′-dihydroxybiphenyl (**9**, 0.37 Å), 4-hydroxybiphenyl (**10**, 0.36 Å), γ-hydroquinone (**19**, 0.27 Å), and resorcinol (**21**, 0.41 Å) have relatively large deviations in unit cell vector lengths. The deviations in distances less than 4 Å are also relatively large (0.18, 0.12, 0.17, and 0.14 Å, respectively).

Aldehydes and Ketones. Ten aldehydes and ketones (**24**−**33**) were used in fitting the gas-phase dipole moments, with two conformers being included for isobutanal. The set of gas-phase compounds contained six straight-chain and three cyclic aliphatic species. The rms deviation between the computed and experimental dipole moments is 0.46 D, the largest deviation being 1.07 D for 1-pyrrolidine carboxaldehyde (**33**, computed 3.40 D versus experimental[41] 4.47 D). Sublimation data for one compound (**34**, 1,4-cyclohexanedione) was employed. The deviation in its lattice energy is 1.6 kcal/mol (calculated −19.7 kcal/mol versus experimental[42] −21.3 kcal/mol). The 11 compounds (**34**−**44**) whose unit cell vectors were included in the fit consist of one cyclic and one acyclic aliphatic ketone, eight aromatic molecules, and one polycyclic aromatic compound (9-anthraldehyde, **41**). In many of the crystals, the crystal symmetry was not preserved upon energy minimization, with deviations of up to 17.7° (for the β angle in 4-hydroxybenzaldehyde, **39**). Three of the compounds (2,4-dihydroxybenzophenone (**35**), 2-hydroxy-5-methylisophthaldehyde (**37**), and 4-hydroxybenzaldehyde (**39**)) exhibit appreciable intermolecular hydrogen bonding between a carbonyl oxygen and hydroxyl hydrogen, with experimental O···H distances of 1.78, 2.13, and 1.72 Å, respectively. The deviations in these computed distances are 0.08, −0.03, and 0.04 Å, respectively, corresponding to an rms deviation of 0.05 Å. The rms deviations in the unit cell vector lengths and angles are 0.43 Å and 3.41°, respectively, while the rms deviation in the interatomic distances less than 4 Å is 0.21 over the 4013 such distances included (an average of 365 per crystal).

Amides. Gas-phase data for four compounds (**45**−**48**), lattice energies for six (**46**−**51**), and unit cell vectors for 21 crystals were used to derive the amide nonbonded energy constants. The lattice energies and dipole moments correspond to essentially the same set used by Hagler, Huler, and Lifson.[15] The rms deviation in dipole moments is 0.12 D, the largest deviation being 0.18 D in acetamide (**45**, computed 3.86 D versus the experimental value of 3.68 D). The compounds used in fitting the lattice energies included both primary and secondary amides as well as a cyclic compound, diketopiperazine (**49**). The rms deviation in lattice energies is 1.6 kcal/mol, with diketopiperazine having the largest deviation, 2.5 kcal/mol (calculated −28.5 versus the experimental value[15] of −26.0 kcal/mol). The observables for the structural properties extends that used by Hagler, Huler, and Lifson.[15] The compounds now include, in addition to the original set, species with double bonds such as crotonamide and *N*-methylsorbamide (**55** and **61**), a triply bonded compound (*N*-methyltetrolamide, **62**), and aromatic compounds such as benzamide (**54**) and *N*-methylbenzamide (**60**). Although each crystal exhibits hydrogen bonding, there is considerable variety among the packing motifs of the various compounds. However, most crystal structures contain either chains or sheets of hydrogen-bonded dimers, as in **II**. The urea

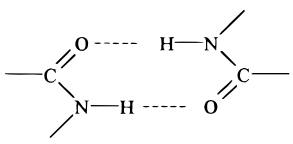

II

crystal is unique in that every hydrogen atom participates in an N−H···O hydrogen bond and each oxygen contributes to four such bonds, two of which come in *perpendicular to the plane of the molecule*.[43] The arrangement of hydrogen bonds about

TABLE 9: Summary of Root-Mean-Square Deviations of CFF-Calculated Energetic and Structural Properties from Experimental Values for All Crystals

		rms deviation			
molecule type	no. of crystals	lattice energy (kcal/mol) (no. crystals)	unit cell length (Å)	unit cell angle (deg)	distance of <4 Å (Å)
alcohols	16		0.21	1.63	0.12
aldehydes & ketones	11	1.60 (1)	0.43	3.41	0.21
amides	21	1.61 (6)	0.50	1.87	0.24
amines	12	0.25 (1)	0.16	1.18	0.13
carboxylic acids	16	3.27 (12)	0.34	2.95	0.20
esters	5		0.44	2.47	0.19
ethers	5		0.33	2.12	0.25
N-heterocycles	7	0.72 (2)	0.61	4.00	0.31
hydrocarbons	25	2.18 (12)	0.23	2.56	0.15
sulfur compounds	18		0.28	2.27	0.15
total/average rms	136	1.60 (34)	0.35	2.45	0.19

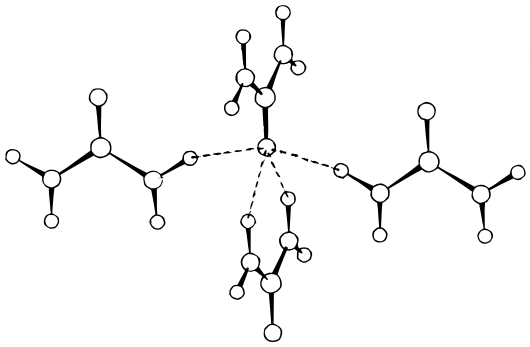

Figure 2. Hydrogen bonding about each oxygen in the urea crystal. The dashed lines represent the hydrogen bonds. The distances vary from 1.92 to 1.99 Å. This shows the unique 4-fold pattern of hydrogen bonding in this crystal.

the oxygen is shown in Figure 2. For all the amides the rms deviation in unit cell lengths is 0.50 Å, in angles is 1.87°, and in distances less than 4 Å is 0.24 Å over the 6049 such distances included (an average of 288 per crystal). The hydrogen bond distances are quite well reproduced, the rms deviation in N−H···O distances being 0.06 Å over the average of 42 unique hydrogen bonds per unit cell in this set of crystals. The deviation in N−H···O angles is 4.0°. The largest deviation in the hydrogen bond length is 0.19 Å, in *N*-methylbenzamide (**60**, computed 2.15 Å versus experimental[44] 1.97 Å). Only two of the crystals (urea and suberamide, **48** and **64**) lose symmetry when their structures are optimized, and the largest such deviation is only 1.4° (in the β angle for suberamide). Overall, the rms deviation is 0.50 Å in cell lengths and 1.9° in cell angles.

Amines. The amine force field parameters were determined from gas-phase dipole moments for 12 amines (including two conformers of ethylamine, **70**), the lattice energy of triethylenediamine (**78**),[38] and the crystal lattice vectors for 12 amine crystals, including four acyclic, seven cyclic aliphatic, and one aromatic amine (aniline, **68**). The rms deviation in dipole moments is 0.14 D, and the largest deviation occurs for quinuclidine (**76,** computed 0.88 D versus experimental[45] 1.20 D). The calculated sublimation energy of triethylenediamine is −14.5 kcal/mol compared to the experimental value[38] of −14.8 kcal/mol. The observables span a range of molecules, some of which exhibit hydrogen bonding, while in others the H-bonding donor is absent. The tertiary amines, for example, exhibit no hydrogen bonding. Thus, in the hexamethylenetetraamine molecule (**86**), which has a cage structure so that no hydrogen bonds are available, the molecules pack in such as way to optimize the van der Waals and polar interactions.[43] Three of the acyclic amines—methylamine, hexamethylenediamine, and ethylenediamine (**72**, **85**, **84**)—have appreciable hydrogen bonding as in **III**. When two amine hydrogen atoms are present,

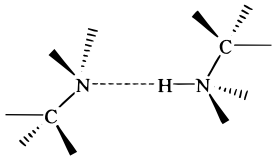

III

generally both participate in hydrogen bonding, although only one of the amine hydrogens in aniline forms a hydrogen bond.[46] The experimental crystal structures contain N···H distances of 2.17 and 2.26 Å in methylamine,[47] 2.21 Å in ethylenediamine,[48] and 2.20 Å in hexamethylenediamine.[49] The computed hydrogen bond distances are shorter in each of the four cases, with the rms deviation being 0.16 Å. The deviation in N−H···N angles is 3.84°. The unit cell vectors of the amines are quite accurately reproduced in the force field calculations (the rms deviation in unit cell distances being 0.16 Å and in angles 1.18°). The short interatomic distances are reproduced to within 0.13 Å rms over the 4770 such distances considered (an average of 398 per crystal). Of the 11 crystal structures calculated, only trimethylamine (**77**) has an rms deviation in the short interatomic distances (0.23 Å) that is greater than 0.20 Å.

Carboxylic Acids. Here, gas-phase dipoles for 8 carboxylic acids, 12 lattice energies, including both polymorphs (α and β) for oxalic acid (**97**), and the structures of these crystals along with malonic acid (**104**), methylmalonic acid (**105**), glycolic acid (**90**), and two aromatic acids, (2,4,6-trimethylbenzoic acid (**102**) and benzoic acid (**103**)), 16 structures in all, were used in the determination of the nonbonded parameters. Only monobasic and dibasic straight-chain acids were employed in fitting dipole moments or lattice energies. Most of these data are the same as used by Lifson, Hagler, and Dauber.[17] The rms deviation between computed and experimental dipole moments is 0.32 D. The largest deviation is found for glycolic acid (**90**), for which the difference is 0.61 D (computed 2.77 D versus experimental[50] 2.16 D). The rms deviation in lattice energies is 3.27 kcal/mol, which is significantly larger than for the other functional groups.

The largest deviations are about 7 kcal/mol for both α- and β-oxalic acid (**97**). The experimental[51] and calculated lattice energies are −24.8 and −31.9 kcal/mol, respectively, for α-oxalic acid and −23.5 and −30.9 kcal/mol, respectively, for β-oxalic acid. (Note, however, that the relative energy difference between the two forms of oxalic acid is well reproduced, the computed result being 1.0 kcal/mol while the experimental value

TABLE 10: Crystal Structures Used in Determining Nonbonded Parameters[a]

crystal	molec[a]	registry no.	ref	crystal	molec[a]	registry no.	ref
			Alcohols				
4,4′-biphenyldiol	9	92-88-6	84	erythritol	17	149-32-6	91
4-biphenylol	10	92-69-3	85	ethanol	6	64-17-5	92
allitol	11	488-44-8	86	galactitol	18	608-66-2	93
catechol	12	120-80-9	87	γ-hydroquinone	19	123-31-9	94
D-glucitol	13	50-70-4	88	pentaerythritol	20	115-77-5	95
D-iditol	14	24557-79-7	86	resorcinol	21	108-46-3	96
D,L-arabinitol	15	6018-27-5	89	ribitol	22	488-81-3	97
D,L-mannitol	16	133-43-7	90	xylitol	23	87-99-0	98
			Aldehydes and Ketones				
1,4-cyclohexanedione	34	637-88-7	99	4-methylbenzophenone	40	134-84-9	105
2,4-dihydroxybenzophenone	35	131-56-6	100	9-anthraldehyde	41	642-31-9	106
2,5-diacetylhydroquinone	36	20129-52-6	101	benzophenone	42	119-61-9	107
2-hydroxy-5-methylisophthalaldehyde	37	7310-95-4	102	diphenylethane-4,4′-dialdehyde	43	1220-08-2	108
4,4′-dimethylbenzophenone	38	611-97-2	103	tetra-*tert*-butylacetone	44	29571-61-7	109
4-hydroxybenzaldehyde	39	123-08-0	104				
			Amides				
3,6-dimethyl-2,5-piperazinedione	52	5625-46-7	110	*N*-methylacetamide	47	79-16-3	118
adipamide	53	628-94-4	111	*N*-methylbenzamide	60	613-93-4	121
benzamide	54	55-21-0	112	*N*-methylsorbamide	61	95702-88-8	121
crotonamide	55	23350-58-5	113	*N*-methyltetrolamide	62	38902-81-7	121
cyclopropanecarboxamide	56	6228-73-5	114	*N*-propyldipropylacetamide	63	2936-11-0	122
decanamide	57	2319-29-1	115	oxamide	51	471-46-5	123
diethylpropionamide	58	55327-21-4	116	suberamide	64	3891-73-4	124
diketopiperazine	49	106-57-0	117	succinamide	65	110-14-5	125
formamide	46	75-12-7	118	*trans*,*trans*-sorbamide	66	821-00-1	126
glutaramide	59	3424-60-0	119	urea	48	57-13-6	127
malonamide	50	108-13-4	120				
			Amines				
1,1,3,6,6,8-hexamethyl-3a,5a,8a,10a-tetraaza-*cis*-10c,10c-perhydropyrene	79	75197-18-1	128	ethylenediamine	84	107-15-3	48
				hexamethylenediamine	85	124-09-4	49
1,3,5-tricyclohexyl-1,3,5-triazacyclohexane	80	6281-14-7	129	hexamethylenetetraamine	86	100-97-0	133
1,4,8,11-tetraazatricyclo[9.3.1.1]hexadecane	81	75920-10-4	130	methylamine	72	74-89-5	47
1,5,9,13-tetraazacyclohexadecane	82	24772-41-6	131	triethylenediamine	78	280-57-9	134
3-azabicyclo[3.2.2]nonane	83	283-24-9	132	trimethylamine	77	75-50-3	135
aniline	68	62-53-3	46				
			Carboxylic Acids				
2,4,6-trimethylbenzoic acid	102	480-63-7	136	malonic acid	104	141-82-2	144
acetic acid	87	64-19-7	137	methylmalonic acid	105	516-05-2	145
adipic acid	95	124-04-9	138	oxalic acid, α and β	97	144-62-7	146
benzoic acid	103	65-85-0	139	propionic acid	93	79-09-4	147
butyric acid	88	107-92-6	140	sebacic acid	98	111-20-6	148
formic acid	89	64-18-6	141	suberic acid	99	505-48-6	149
glutaric acid	96	110-94-1	142	succinic acid	100	110-15-6	150
glycolic acid	90	79-14-1	143	valeric acid	101	109-52-4	151
			Esters				
1,2,3,4-cyclobutanetetracarboxylic acid tetramethyl ester	110	1032-95-7	152	γ-D-galactonolactone	112	2782-07-2	154
				mesotartaric acid dimethyl ester	113	5057-96-5	155
D-12-hydroxyoctadecanoic acid methyl ester	111	141-23-1	153	phenyl benzoate	114	93-99-2	156
			Ethers				
1,3,5-trioxane	122	110-88-3	157	diethyl ether	115	60-29-7	160
1,4-dioxane, **I** and **II**	123	123-91-1	158	trimethylene oxide	121	503-30-0	161
adamantylideneadamantane epoxide	124	29186-07-0	159				
			N-Heterocycles				
1,5-naphthyridine	130	254-79-5	162	2,6-naphthyridine	134	253-50-9	162
1,8-naphthyridine	131	254-60-4	163	imidazole	128	288-32-4	55
2,2′-bipyridine	132	366-18-7	164	pyrimidine	129	289-95-2	166
2,2′-dipyridylamine	133	1202-34-2	165				
			Hydrocarbons				
1,4-di-*tert*-butylbenzene	148	1012-72-2	167	hexacyclohexadecane	157	53527-53-0	177
1-biadamantane	149	29542-62-9	168	hexaethylbenzene	158	604-88-6	178
1-biapocamphane	150	18313-41-2	168	naphthalene	143	91-20-3	179
adamantane	136	281-23-2	57	*n*-hexane	140	110-54-3	180
anthracene	137	120-12-7	169	*n*-octane	141	111-65-9	181
benzene	138	71-43-2	170	*n*-pentane	142	109-66-0	181
bicyclopropyl	151	5685-46-1	171	ovalene	144	190-26-1	182
biphenyl	152	92-52-4	172	perylene	145	198-55-0	183
chrysene	139	218-01-9	58	phenanthrene	146	85-01-8	184
coronene	153	191-07-1	173	pyrene	159	129-00-0	185
durene	154	95-93-2	174	*trans*,*trans*-1,3,5,7-octatetraene	160	1482-91-3	186
ethane	155	74-84-0	175	triphenylene	147	217-59-4	187
ethylene	156	74-85-1	176				

TABLE 10: (Continued)

crystal	molec[a]	registry no.	ref	crystal	molec[a]	registry no.	ref
		Sulfur Compounds					
1,2,5,6,9,10-hexathiacyclododecane	163	100189-77-3	188	dibenzyl disulfide	171	150-60-7	197
1,3,5-trithiane	164	291-21-4	189	dibenzylpentathiane	172	59597-70-5	198
1,4,8,11-tetrathiacyclotetradecane	165	24194-61-4	190	dithia[3.3.1]propellane	173	21533-67-5	199
2,11,20,29-tetrathia[3.3.3.3]parabenzophane	166	60742-99-6	191	dithia[3.3.3]propellane	174	32681-86-0	199
2,4,6-trimethyl-1,3,5-trithiane, α	167	2765-04-0	192	hexathiepane	175	17233-71-5	198
2,4,6-trimethyl-1,3,5-trithiane, β	167	2765-04-0	193	orthorhombic sulfur, α	176	10544-50-0	200
2,6,15,19-tetrathia[7.7]paracyclophane	168	26822-25-3	194	pentathiane	177	18091-79-7	198
3,10-dithiabicyclo[10.2.2]hexadeca-12,14(1),15-triene	169	28667-58-5	195	tetraphenylorthothiocarbonate	178	14758-47-5	201
7,8,9,16,17,18-hexathiadispiro[5.3.5.3]octadecane	170	71766-22-8	196	*trans*-1,4,5,8-tetrathiadecalin	179	111727-91-4	202

[a] α and β or **I** and **II** denote different polymorphic forms.

is 1.3 kcal/mol.) Further analysis shows that the lattice energies computed at the experimental crystal structures, which were used to derive the nonbond parameters, are −25.6 and −26.6 kcal/mol for the α and β polymorphs, respectively, in reasonable agreement with the experimental values. The latter computed energies are also close to the results, −25.2 kcal/mol for both polymorphs, found by Lifson, Hagler, and Dauber[17] in their derivation of the nonbonded parameters at the experimental crystal structures.

When the atomic partial charges are determined from ab initio calculations, it is found that the charge on the carbonyl oxygen is appreciably more negative in oxalic acid than in larger carboxylic acids such as succinic acid. These partial charges in the force field, which were developed primarily using the larger acids, are therefore somewhat too negative when applied to oxalic acid. Since the lattice energy of oxalic acid at the experimental crystal structure is already too negative, when the crystal is optimized, it becomes still more negative. This appears to be the reason for the present 7 kcal/mol deviations between computed and experimental lattice energies for these two crystals.

If the deviations in the energies for the oxalic acid polymorphs are excluded, the average rms deviation decreases to 1.53 kcal/mol. The lattice energies of the monoacids are all predicted more accurately (rms deviation of <0.5 kcal/mol) than the diacids (rms deviation of ∼2.0 kcal/mol).

The intrachain structures of crystals of carboxylic acids, particularly the dibasic acids, are generally dominated by intermolecular hydrogen bonding. Intermolecular hydrogen bonds are short (1.6−1.8 Å) and generally involve two hydrogen bonds within each pair of carboxylic acid groups (**IV**). In dibasic

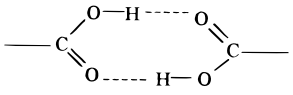

IV

acids, hydrogen bonding usually leads to the formation of cyclic dimers, as in adipic (**95**), glutaric (**96**), methylmalonic (**105**), and β-oxalic (**97**) acids. However, α-oxalic acid (and monobasic acids such as formic and acetic) form chains in which only a single C═O···H hydrogen bond connects adjacent molecules, as for example in **V**. Such structures have been termed catamers.[39,44,52] Overall, the rms deviations in the unit cell vector lengths and angles of the carboxylic acid crystals are 0.34 Å and 2.95°, respectively, and the deviation in interatomic distances less than 4 Å is 0.20 Å over 3473 such distances (an average of 204 per crystal). Two of the crystals (butyric acid and propionic acid, **88** and **93**) lose symmetry upon optimization, with the largest deviation (from 90°) being 7.41° in the α angle for butyric acid. The O···H hydrogen bond distances are well reproduced in the calculated crystal structures, the rms deviation

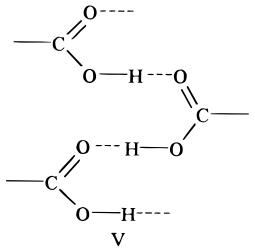

V

being 0.08 Å. The computed distance is too long in 80% of the hydrogen bonds. The largest deviation, 0.13 Å, occurs for the shortest distance, which is found in methylmalonic acid (**105**, computed 1.73 Å versus experimental[39] value 1.60 Å). The structures of the mono- and diacids are predicted equally well. For example, the rms deviation in the short interatomic distances is 0.19 Å for the diacids and 0.20 for the monoacids. α-Oxalic acid and 2,4,6-trimethylbenzoic acid (**102**) display large deviations in unit cell vectors (0.56 and 0.52 Å, respectively), even though they have small rms deviations (0.21 and 0.20 Å) in the short interatomic distances. This shows that examination of either unit cell vectors or interatomic distances alone is not a sufficient measure of the accuracy of the model.

Esters. Gas-phase dipole moment data for four esters (**106**−**109**) and crystal lattice vectors for five (**110**−**114**) were included in the parametrization. No lattice energies of esters were available. Dipole moments of both gauche and trans conformers of ethyl formate (**106**) were included. The rms deviation in dipole moments is 0.17 D, with the largest deviation, 0.23 D, occurring for γ-valerolactone (**107**, calculated to be 4.48 D as opposed to the experimental value[53] of 4.71 D). The crystals span molecules containing two straight-chain esters (mesotartaric acid dimethyl ester **113**, and 12-hydroxyoctadecanoic acid methyl ester **111**), two saturated ring compounds (1,2,3,4-cyclobutanetetracarboxylic acid tetramethyl ester **110**, and γ-galactonolactone **112**), and one aromatic (phenyl benzoate **114**), representing a variety of intermolecular environments. The resulting rms deviation in distances less than 4 Å for this set of crystals is 0.19 Å over 2287 such distances (an average of 457 per crystal). Three of these compounds (mesotartaric acid dimethyl ester, 12-hydroxyoctadecanoic acid methyl ester, and γ-galactonolactone) also contain hydroxyl groups and engage in appreciable hydrogen bonding. The rms deviation in O···H hydrogen bond distances for these species is 0.12 Å, with no systematic deviation. Since these are bifunctional compounds, containing both a carbonyl and an alcohol hydroxyl group, it is interesting to compare the hydrogen bond distances with those in the monofunctional acids and alcohols. The deviation in hydrogen bond lengths in the bifunctional compounds (0.12 Å) is somewhat larger than in the alcohols (0.05 Å) or acids (0.08 Å). Three of the five compounds lose their symmetries when their structures are optimized, although the largest deviation

from symmetry is only 0.4° (in the β angle for phenyl benzoate). For the five esters considered, the rms deviations in the unit cell lengths and angles are 0.44 Å and 2.47°.

Ethers. Gas-phase dipole moment data for seven ethers and crystal lattice vectors from six, including two polymorphs of 1,4-dioxane (**123**), were used for this family. The dipole moments are not fit as well as for most of the other families, the rms deviation being 0.33 D. The largest deviation, 0.60 D, occurs for trimethyleneoxide (**121**, computed 1.34 D versus experimental[37] 1.94 D). The crystals are highly diverse and include, for example, diethyl ether (**115**), 1,3,5-trioxane (**122**), and an epoxide (**124**). The rms deviation in intermolecular distances less than 4 Å is 0.25 Å over 1559 such distances (an average of 312 per crystal). The largest rms deviation, 0.66 Å, is found for one of the polymorphs (**I**) of 1,4-dioxane (**123**). Interestingly, the structure of polymorph **II** is reproduced considerably more accurately, with an rms deviation of only 0.15 Å and with correspondingly smaller rms deviations in unit cell lengths and angles. None of these compounds contain polar hydrogen atoms, so there is no hydrogen bonding, and the crystal packing is determined by other nonbonded interactions. The rms deviations in the unit cell vector lengths and angles are 0.33 Å and 2.12°, respectively. Only 1,3,5-trioxane (**122**) loses symmetry when its crystal structure is optimized, and the difference is only 1.21° in both the α and β angles, α increasing to 91.21° and β decreasing to 89.79°.

N-Heterocycles. Gas-phase dipole moment data for three heterocyclic compounds (1,3,4-oxadiazole, pyridine, and pyrrole **125**−**127**), lattice energies for two (imidazole and pyrimidine **128**−**129**), and crystal structures of seven compounds, including one five-membered ring (imidazole), one six-membered ring (pyrimidine), and three bicyclic compounds (naphthyridines **130** , **131**, and **134**, also referred to as diazanaphthalenes) were used to refine the potential function. The rms deviation in dipole moments is 0.21 D, the largest deviation of 0.33 D occurring for 1,3,4-oxadiazole (**125**, 3.37 D calculated versus an experimental value[37] of 3.04 D). The calculated lattice energies are −20.7 and −12.1 kcal/mol compared to the experimental values of −20.5 and −13.1 kcal/mol for imidazole[42] and pyrimidine,[54] respectively. The lattice energy of imidazole is much lower than that of pyrimidine, as would be expected from the occurrence of intermolecular hydrogen bonds in imidazole, which cannot form in pyrimidine crystals.[55] The rms deviations in unit cell lengths and angles are 0.61 Å and 4.00°, respectively, and the deviation in interatomic distances less than 4 Å is 0.31 Å over the 1749 such distances (an average of 250 per crystal). All the crystals maintained their symmetries either exactly or very closely during the optimization, the largest deviation from the value of the unit cell angle required by the experimental symmetry being 0.06° (in the γ angle of 1,5-naphthyridine **130**). In terms of unit cell lengths, angles, and nonbonded distances, this is the least accurately modeled of the 11 types of molecules. However, the rms deviation in lattice energies, 0.72 kcal/mol, is the second smallest among the species (albeit sampled over only two values).

Hydrocarbons. The hydrocarbons, being extremely nonpolar, in general have very small dipole moments. Only one experimental dipole (toluene **135**) was available. Lattice energies of 12 hydrocarbon molecules were included in the data set, as well as 24 crystal structures. The lattice energies included three straight-chain compounds (*n*-hexane, *n*-octane, and *n*-pentane **140**, **141**, and **142**), one cage structure (adamantane **136**), and five aromatic compounds ranging from benzene (**138**) to ovalene (**144**), which has 10 fused rings. The rms deviation in lattice energies is 2.18 kcal/mol and is nearly independent of the type of molecule, although the aliphatic compounds are fit slightly better than the aromatic ones. The largest deviation is 4.2 kcal/mol for perylene (**145**, computed −31.7 kcal/mol versus experimental[56] −35.7 kcal/mol). The crystals spanned structures including straight-chain alkanes and alkenes, cage structures, and aromatic compounds, again ranging from benzene to ovalene (**144**). These display a wide variety of packing motifs, ranging from the simple fcc crystal structure seen for adamantane (**136**), due to its nearly spherical molecular shape,[43,57] to the oriented molecules arranged in coplanar sheets seen in crystals of polyaromatic compounds such as chrysene (**139**).[58] The rms deviations for the unit cell vector lengths and angles are 0.23 Å and 2.56°, respectively, and the deviation in interatomic distances less than 4 Å is 0.15 Å over 9521 such distances (an average of 381 per crystal). Saturated and unsaturated hydrocarbons are modeled about equally well. For example, the rms deviations in unit cell lengths and angles for ethane (**155**) are 0.22 Å and 0.63°, respectively, compared to 0.13 Å and 0.10° for ethylene (**156**) and 0.18 Å and 0.00° for benzene (**138**). Also, the crystal structures of the large molecules are computed about as accurately as the smaller ones, as can be seen by comparing the benzene values with those of coronene (**153**, seven fused rings) for which the rms deviations in unit cell lengths and angles are 0.15 Å and 0.60°.

Sulfur Compounds. The experimental observables for this family included dipole moments for two sulfur compounds, 1,3,4-thiadiazole (**161**) and thiophene (**162**).[37] The crystal structures of 18 sulfur compounds in the data set were chosen to represent a range of molecular topologies and packing motifs. All contain C−S−C and/or S−S−C and/or S−S−S linkages. They include sulfur in rings, such as orthorhombic sulfur (S_8 **176**), sulfur atoms within saturated hydrocarbon rings, as in 1,3,5,-trithiane (**164**), disulfide linkages within saturated hydrocarbons rings as in 7,8,9,16,17,18-hexathiadispiro[5.3.5.3]-octadecane (**170**), and sulfur connected to a benzene ring, as in tetraphenylorthiothiocarbonate (**178**). The deviations in calculated dipole moments are 0.28 D (3.01 D versus experimental 3.29 D) and 0.27 D (0.82 D versus experimental 0.55 D), respectively. No lattice energies were available. The rms deviations for the unit cell lengths and angles are 0.28 Å and 2.27°, respectively, and the deviation in interatomic distances less than 4 Å is 0.15 Å over 4714 such distances (an average of 262 per crystal). Each of the crystals maintained the correct symmetry during energy minimization except 1,4,5,8-tetrathiadecalin (**179**), for which the angle β increased by 5° to 95°. Orthorhombic sulfur (S_8 **176**) and dithia[3.3.1]propellane (**173**) have relatively large deviations in unit cell lengths (0.32 and 0.43 Å, respectively), even though they have small deviations in the short interatomic distances (only 0.09 and 0.13 Å, respectively). In both cases, the packing is responsible for this apparent inconsistency, since there are eight orthorhombic sulfurs and four dithia[3.3.1]propellane molecules along one unit cell vector of their respective crystals. Thus, the deviations in unit cell vectors will be 8 and 4 times, respectively, the deviations in the intermolecular distances along these directions.

Conclusions

In this paper we have described the derivation of a set of atomic partial charge parameters and van der Waals coefficients by fitting the lattice energies of 34 crystals, structures of 136 crystals, and gas-phase dipole moments of 63 molecules. The values of the resulting parameters were reported for 16 atom types. These are sufficient to model all the compounds

considered, which included alcohols, aldehydes, amides, amines, acids, esters, ethers, ketones, nitrogen heterocyclic compounds, hydrocarbons (saturated aliphatic, unsaturated aliphatic, and aromatic), and a set of sulfur compounds. These parameters are employed in the current CFF force field and were also used in deriving the CFF valence terms.[1−6] Tests were carried out to determine the most accurate form of the nonbonded potential, using as criteria the deviations between the computed and experimental values of the crystal lattice energies, unit cell lengths, unit cell angles, and interatomic distances less than 4 Å between molecules. These tests showed that, as seen in earlier studies, a van der Waals potential of the "9-6" form using Waldman-Hagler combination rules gave appreciably more accurate results than using arithmetic−geometric mean combination rules. The accuracies of the predicted dipole moments, crystal lattice energies, and crystal lattice vectors are remarkably similar among the functional groups and packing motifs considered. Although many different types of hydrogen bonds are formed in the differing families of molecular crystals we examined, overall in most families no systematic deviation in the computed hydrogen bond lengths was seen. Significant deviations remain, however, such as the 2.39 kcal/mol rms deviation in lattice energies (due largely to the 3.27 kcal/mol deviation in carboxylic acids). The present results provide a large data set against which other parameters and functional forms can be tested. It is likely that this is close to the limit of the accuracy that can be achieved with the simple functional forms (spherically symmetric potentials about each atom) given in eqs 1 and 4. We believe that further development in this area will require more realistic functional forms for the nonbond potential, such as inclusion of charge anisotropy and polarizability.

Acknowledgment. The authors thank Dr. Marvin Waldman for several helpful suggestions and for carefully reviewing this manuscript. This work was supported by the Potential Energy Functions Consortium.

References and Notes

(1) Peng, Z.; Ewig, C. S.; Hwang, M.-J.; Waldman, M.; Hagler, A. T. *J. Phys. Chem. A* **1997**, *101*, 7243−7252.

(2) Maple, J. R.; Hwang, M.-J.; Jalkanen, K. J.; Stockfisch, T. P.; Hagler, A. T. *J. Comput. Chem.* **1998**, *19*, 430−458.

(3) Hwang, M.-J.; Ni, X.; Waldman, M.; Ewig, C. S.; Hagler, A. T. *Biopolymers* **1998**, *45*, 435−468.

(4) Maple, J. R.; Hwang, M.-J.; Stockfisch, T. P.; Dinur, U.; Waldman, M.; Ewig, C. S.; Hagler, A. T. *J. Comput. Chem.* **1994**, *15*, 162−182.

(5) Hwang, M.-J.; Stockfisch, T. P.; Hagler, A. T. *J. Am. Chem. Soc.* **1994**, *116*, 2515−2525.

(6) Maple, J. R.; Hwang, M.-J.; Stockfisch, T. P.; Hagler, A. T. *Isr. J. Chem.* **1994**, *34*, 195−231.

(7) Jorgensen, W. L. *J. Am. Chem. Soc.* **1981**, *103*, 335−340.

(8) Jorgensen, W. L.; Tirado-Rives, J. *J. Am. Chem. Soc.* **1988**, *110*, 1657−1667.

(9) Pranata, J.; Wierschke, S. G.; Jorgensen, W. L. *J. Am. Chem. Soc.* **1991**, *113*, 2810−2819.

(10) Halgren, T. A. *J. Comput. Chem.* **1996**, *17*, 520−552.

(11) Hill, J.-R. *J. Comput. Chem.* **1997**, *18*, 211−220.

(12) Williams, D. E. *J. Chem. Phys.* **1967**, *47*, 4680−4684.

(13) Warshel, A.; Lifson, S. *J. Chem. Phys.* **1970**, *53*, 582−594.

(14) Hagler, A. T.; Lifson, S. *Acta Crystallogr.* **1974**, *B30*, 1336−1341.

(15) Hagler, A. T.; Huler, E.; Lifson, S. *J. Am. Chem. Soc.* **1974**, *96*, 5319−5327.

(16) Hagler, A. T.; Lifson, S. *J. Am. Chem. Soc.* **1974**, *96*, 5327−5335.

(17) Lifson, S.; Hagler, A. T.; Dauber, P. *J. Am. Chem. Soc.* **1979**, *101*, 5111−5121.

(18) Hagler, A. T.; Lifson, S.; Dauber, P. *J. Am. Chem. Soc.* **1979**, *101*, 5122−5130.

(19) Dillen, J. L. M. *J. Comput. Chem.* **1995**, *16*, 610−619.

(20) Momany, F. A.; Carruthers, L. M.; McGuire, R. F.; Scheraga, H. A. *J. Phys. Chem.* **1974**, *78*, 1595−1620.

(21) Momany, F. A.; Carruthers, L. M.; Scheraga, H. A. *J. Phys. Chem.* **1974**, *78*, 1621−1630.

(22) Dauber-Osguthorpe, P.; Roberts, V. A.; Osguthorpe, D. J.; Wolff, J.; Genest, M.; Hagler, A. T. *Proteins: Struct. Funct. Genet.* **1988**, *4*, 31−47.

(23) Weiner, S. J.; Kollman, P. A.; Case, D. A.; Singh, U. C.; Ghio, C.; Alagona, G.; Profeta, S., Jr.,; Weiner, P. *J. Am. Chem. Soc.* **1984**, *106*, 765−784.

(24) Weiner, S. J.; Kollman, P. A.; Nguyen, D. T.; Case, D. A. *J. Comput. Chem.* **1986**, *7*, 230−252.

(25) Cornell, W. D.; Cieplak, P.; Bayly, C. I.; Gould, I. R.; Merz, K. M., Jr.; Ferguson, D. M.; Spellmeyer, D. C.; Fox, T.; Caldwell, J. W.; Kollman, P. A. *J. Am. Chem. Soc.* **1995**, *117*, 5179−5197.

(26) Rossky, P. J.; Karplus, M.; Rahman, A. *Biopolymers* **1979**, *18*, 825−854.

(27) Brooks, B. R.; Bruccoleri, R. E.; Olafson, B. D.; States, D. J.; Swaminathan, S.; Karplus, M. *J. Comput. Chem.* **1983**, *4*, 187−217.

(28) Nilsson, L.; Karplus, M. *J. Comput. Chem.* **1986**, *7*, 591−616.

(29) MacKerrell, A. D., Jr.; Bashford, D.; Bellott, M.; Dunbrack, R. L., Jr.; Evanseck, J. D.; Field, M. J.; Fischer, S.; Gao, J.; Guo, H.; Ha, S.; Joseph-McCarthy, D.; Kuchnir, L.; Kuczera, K.; Lau, F. T. K.; Mattos, C.; Michnick, S.; Ngo, T.; Nguyen, D. T.; Prodhom, B.; Reiher, W. E., III; Roux, B.; Schlenkrich, M.; Smith, J. C.; Stote, R.; Straub, J.; Watanabe, M.; Wiorkiewicz-Kuczera, J.; Yin, D.; Karplus, M. *J. Phys. Chem. B* **1998**, *102*, 3586−3616.

(30) Hagler, A. T.; Ewig, C. S. *Comput. Phys. Commun.* **1994**, *84*, 131−155.

(31) Sun, H.; Mumby, S. J.; Maple, J. R.; Hagler, A. T. *J. Am. Chem. Soc.* **1994**, *116*, 2978−2987.

(32) Meier, R. J.; Maple, J. R.; Hwang, M.-J.; Hagler, A. T. *J. Phys. Chem.* **1995**, *99*, 5445−5456.

(33) Sun, H.; Mumby, S. J.; Maple, J. R.; Hagler, A. T. *J. Am. Chem. Soc.* **1994**, *116*, 2978−2987.

(34) Waldman, M.; Hagler, A. T. *J. Comput. Chem.* **1993**, *14*, 1077−1084.

(35) Shipman, L. L.; Burgess, A. W.; Scheraga, H. A. *J. Phys. Chem.* **1976**, *80*, 52−54.

(36) *Vibgeom Manual*; Molecular Simulations Inc.: San Diego, CA, 1993.

(37) Nelson, R. D., Jr.; Lide, D. R., Jr.; Maryott, A. A. *Selected Values of Electric Dipole Moments for Molecules in the Gas Phase*; National Bureau of Standards: Washington, DC, 1967.

(38) Cox, J. D.; Pilcher, G. *Thermochemistry of Organic and Organometallic Compounds*; Academic Press: London, 1970.

(39) Hagler, A. T.; Dauber, P.; Lifson, S. *J. Am. Chem. Soc.* **1979**, *101*, 5131−5141.

(40) MacDonald, J. N.; Norbury, D.; Sheridan, J. *J. Chem. Soc., Faraday Trans. 2* **1978**, *74*, 1365−1375.

(41) Lee, S. G.; Hwang, K. W.; Bohn, R. K.; Hillig, K. W.; Kuczkowski, R. L. *Acta Chem. Scand.* **1988**, *A42*, 603−610.

(42) De Wit, H. G. M.; Van Miltenburg, J. C.; De Kruif, C. G. *J. Chem. Thermodyn.* **1983**, *15*, 651−663.

(43) Mak, T. C. W.; Zhou, G.-D. *Crystallography in Modern Chemistry: A Resource Book of Crystal Structures*; John Wiley & Sons: New York, 1992.

(44) Leiserowitz, L. *Acta Crystallogr.* **1976**, *B32*, 775−802.

(45) Lassier, B.; Brot, C.; Dat-Xuong, N. *Mol. Phys.* **1974**, *27*, 1697−1700.

(46) Fukuyo, M.; Hirotsu, K.; Higuchi, T. *Acta Crystallogr.* **1982**, *B38*, 640−643.

(47) Atoji, M.; Lipscomb, W. N. *Acta Crystallogr.* **1953**, *6*, 770−774.

(48) Jamet-Delcroix, S. *Acta Crystallogr.* **1973**, *B29*, 977−980.

(49) Binnie, W. P.; Robertson, J. M. *Acta Crystallogr.* **1950**, *3*, 424−429.

(50) Blom, C. E.; Bauder, A. *Chem. Phys. Lett.* **1981**, *82*, 492−495.

(51) de Wit, H. G. M.; Bouwstra, J. A.; Blok, J. G.; de Kruif, C. G. *J. Chem. Phys.* **1983**, *78*, 1470−1475.

(52) Berney, C. V. *J. Am. Chem. Soc.* **1973**, *95*, 708−716.

(53) Alonso, J. L.; Gonzalez, E.; Caminati, W.; Velino, B. *J. Mol. Spectrosc.* **1987**, *122*, 247−258.

(54) Nabavian, M.; Sabbah, R.; Chastel, R.; Laffitte, M. *J. Chim. Phys. Phys.-Chim. Biol.* **1977**, *74*, 115−126.

(55) McMullan, R. K.; Epstein, J.; Ruble, J. R.; Craven, B. M. *Acta Crystallogr.* **1979**, *B35*, 688−691.

(56) Gigli, R.; Malaspina, L.; Bardi, G. *Ann. Chim.* **1973**, *63*, 627−633.

(57) Nordman, C. E.; Schmitkons, D. L. *Acta Crystallogr.* **1965**, *18*, 764−767.

(58) Burns, D. M.; Iball, J. *Proc. R. Soc. London* **1960**, *A257*, 491−514.

(59) Kondo, S.; Hirota, E. *J. Mol. Spectrosc.* **1970**, *34*, 97−107.

(60) Macdonald, J. N.; Norbury, D.; Sheridan, J. *Spectrochim. Acta* **1978**, *34A*, 815−818.

(61) Bhaumik, A.; Brooks, W. V. F.; Dass, S. C.; Sastry, K. V. L. N. *Can. J. Chem.* **1970**, *48*, 2949−2954.

(62) Pierce, L.; Chang, C. K.; Hayashi, M.; Nelson, R. *J. Mol. Spectrosc.* **1967**, *32*, 449−457.
(63) Wolf, K. L.; Gross, W. J. *Z. Phys. Chem.* **1931**, *B14*, 305−325.
(64) Scharpen, L. H.; Laurie, V. W. *J. Chem. Phys.* **1968**, *49*, 221−228.
(65) Kim, H.; Gwinn, W. D. *J. Chem. Phys.* **1969**, *51*, 1815.
(66) Stiefvater, O. L. *Z. Naturforsch.* **1986**, *41a*, 641.
(67) Kojima, T.; Yano, E.; Nakagawa, K.; Tsunekawa, S. *J. Mol. Spectrosc.* **1987**, *122*, 408−416.
(68) Fischer, E.; Botskor, I. *J. Mol. Spectrosc.* **1982**, *91*, 116−127.
(69) Mehrotra, S. C.; Griffin, L. L.; Britt, C. O.; Boggs, J. E. *J. Mol. Spectrosc.* **1977**, *64*, 244−251.
(70) McClellan, A. L. *Table of Experimental Dipole Moments*; Rahara Press: El Cerrito, 1974; Vol. 2.
(71) Marstokk, K.-M.; Møllendal, H. *J. Mol. Struct.* **1973**, *15*, 137−50.
(72) Bolton, K.; Lister, D. G.; Sheridan, J. *J. Chem. Soc., Faraday Trans. 2* **1974**, *70*, 113−123.
(73) Marstokk, K.-M.; Møllendal, H. *J. Mol. Struct.* **1974**, *20*, 257−267.
(74) Riveros, J. M.; Wilson, E. B., Jr. *J. Chem. Phys.* **1967**, *46*, 4605−4612.
(75) Seki, S.; Suzuki, K.; Koide, T. *Kogyo Kagaku Zasshi* **1956**, *77*, 346.
(76) Bauder, A.; Günthard, H. H. *Helv. Chim. Acta* **1958**, *41*, 670−673.
(77) Davies, M.; Jones, A. H. *Trans. Faraday Soc.* **1959**, *55*, 1329.
(78) Egan, E. P., Jr.; Wakefield, Z. T.; Farr, T. D. *J. Chem. Eng. Data* **1965**, *10*, 138−140.
(79) Suzuki, K.; Onishi, S.; Koide, T.; Seki, S. *Bull. Chem. Soc. Jpn.* **1956**, *29*, 127−131.
(80) Bradley, R. S.; Cotson, S. *J. Chem. Soc.* **1953**, 1684−1688.
(81) Jochems, R.; Dekker, H.; Mosselman, C.; Somsen, G. *J. Chem. Thermodyn.* **1982**, *14*, 395−398.
(82) De Kruif, C. G. *J. Chem. Thermodyn.* **1980**, *12*, 243−248.
(83) Alberty, R. A.; Chung, M. B.; Reif, A. K. *J. Phys. Chem. Ref. Data* **1990**, *19*, 349−370.
(84) Jackisch, M. A.; Fronczek, F. R.; Geiger, C. C.; Hale, P. S.; Daly, W. H.; Butler, L. G. *Acta Crystallogr.* **1990**, *C46*, 919−922.
(85) Brock, C. P.; Haller, K. L. *J. Phys. Chem.* **1984**, *88*, 3570−3574.
(86) Azarnia, N.; Jeffrey, G. A.; Shen, M. S. *Acta Crystallogr.* **1972**, *B28*, 1007−1013.
(87) Brown, C. J. *Acta Crystallogr.* **1966**, *21*, 170−174.
(88) Park, Y. J.; Jeffrey, G. A.; Hamilton, W. C. *Acta Crystallogr.* **1971**, *B27*, 2393−2401.
(89) Hunter, F. D.; Rosenstein, R. D. *Acta Crystallogr.* **1968**, *B24*, 1652−1660.
(90) Kanters, J. A.; Roelofsen, G.; Smits, D. *Acta Crystallogr.* **1977**, *B33*, 3635−3640.
(91) Ceccarelli, C.; Jeffrey, G. A.; McMullan, R. K. *Acta Crystallogr.* **1980**, *B36*, 3079−3083.
(92) Jönsson, P.-G. *Acta Crystallogr.* **1976**, *B32*, 232−235.
(93) Berman, H. M.; Rosenstein, R. D. *Acta Crystallogr.* **1968**, *B24*, 435−441.
(94) Maartmann-Moe, K. *Acta Crystallogr.* **1966**, *21*, 979−982.
(95) Eilerman, D.; Rudman, R. *Acta Crystallogr.* **1979**, *B35*, 2458−2460.
(96) Bacon, G. E.; Lisher, E. J. *Acta Crystallogr.* **1980**, *B36*, 1908−1916.
(97) Kim, H. S.; Jeffrey, G. A.; Rosenstein, R. D. *Acta Crystallogr.* **1969**, *B25*, 2223−2230.
(98) Kim, H. S.; Jeffrey, G. A. *Acta Crystallogr.* **1969**, *B25*, 2607−2613.
(99) Mossel, A.; Romers, C. *Acta Crystallogr.* **1964**, *17*, 1217−1223.
(100) Liebich, B. W. *Acta Crystallogr.* **1979**, *B35*, 1186−1190.
(101) Wajsman, E.; Grabowski, M. J.; Stepien, A.; Cygler, M. *Cryst. Struct. Commun.* **1978**, *7*, 233−236.
(102) Ray, T.; Gupta, S. *Cryst. Struct. Commun.* **1982**, *11*, 59−63.
(103) Kojic-Prodic, B.; Bresciani-Pahor, N.; Horvatic, D. *Acta Crystallogr.* **1990**, *C46*, 430−432.
(104) Iwasaki, F. *Acta Crystallogr.* **1977**, *B33*, 1646−1648.
(105) Kutzke, H.; Al-Mansour, M.; Klapper, H. *J. Mol. Struct.* **1996**, *374*, 129−135.
(106) Trotter, J. *Acta Crystallogr.* **1959**, *12*, 922−928.
(107) Fleischer, E. B.; Sung, N.; Hawkinson, S. *J. Phys. Chem.* **1968**, *78*, 4311−4312.
(108) Celikel, R.; Geddes, A. J.; Sheldrick, B. *Cryst. Struct. Commun.* **1978**, *7*, 683−688.
(109) Lepicard, G.; Berthou, J.; Delettré, J.; Laurent, A.; Mornon, J.-P. *C. R. Acad. Sci.* **1973**, *276*, 575−578.
(110) Groth, P. *Acta Chem. Scand.* **1969**, *23*, 3155−3162.
(111) Hospital, M.; Housty, J. *Acta Crystallogr.* **1966**, *20*, 626−630.
(112) Blake, C. C. F.; Small, R. W. H. *Acta Crystallogr.* **1972**, *B28*, 2201−2206.
(113) Shimizu, S.; Kekka, S.; Kashino, S.; Haisa, M. *Bull. Chem. Soc. Jpn.* **1974**, *47*, 1627−1631.
(114) Long, R. E.; Maddox, H.; Trueblood, K. N. *Acta Crystallogr.* **1969**, *B25*, 2083−2094.
(115) Brathovde, J. R.; Lingafelter, E. C. *Acta Crystallogr.* **1958**, *11*, 729−732.
(116) Cohen-Addad, C.; D'Assenza, G.; Tailladier, G.; Benoit-Guyod, J. L. *Acta Crystallogr.* **1975**, *B31*, 835−841.
(117) Degeilh, R.; Marsh, R. E. *Acta Crystallogr.* **1959**, *12*, 1007.
(118) Ottersen, T. *Acta Chem. Scand.* **1975**, *A29*, 939−944.
(119) Hospital, M.; Housty, J. *Acta Crystallogr.* **1966**, *21*, 413−418.
(120) Chieh, P. C.; Subramanian, E.; Trotter, J. *J. Chem. Soc. A* **1970**, 179−184.
(121) Leiserowitz, L.; Tuval, M. *Acta Crystallogr.* **1978**, *B34*, 1230−1247.
(122) Cohen-Addad, C.; Grand, A. *Acta Crystallogr.* **1974**, *B30*, 1342−1346.
(123) Ayerst, E. M.; Duke, J. R. C. *Acta Crystallogr.* **1954**, *7*, 588−590.
(124) Hospital, M.; Housty, J. *Acta Crystallogr.* **1966**, *20*, 368−373.
(125) Davies, D. R.; Pasternak, R. A. *Acta Crystallogr.* **1956**, *9*, 334−340.
(126) Filippakis, S. E.; Leiserowitz, L.; Schmidt, G. M. J. *J. Chem. Soc. B* **1967**, 297−304.
(127) Swaminathan, S.; Craven, B. M.; McMullan, R. K. *Acta Crystallogr.* **1984**, *B40*, 300−306.
(128) Gluzinski, P.; Krajewski, J. W.; Urbanczyk-Lipkowska, Z. *Acta Crystallogr.* **1980**, *B36*, 2182−2184.
(129) Bouchemma, A.; McCabe, P. H.; Sim, G. A. *Acta Crystallogr.* **1988**, *C44*, 1469−1472.
(130) Gabe, E. J.; Le Page, Y.; Prasad, L.; Weisman, G. R. *Acta Crystallogr.* **1982**, *B38*, 2752−2754.
(131) Smith, W. L.; Ekstrand, J. D.; Raymond, K. N. *J. Am. Chem. Soc.* **1978**, *100*, 3539−3544.
(132) Amzel, L. M.; Baggio, S.; Baggio, R. F.; Becka, L. N. *Acta Crystallogr.* **1974**, *B30*, 2494−2496.
(133) Stevens, E. D.; Hope, H. *Acta Crystallogr.* **1975**, *A31*, 494−498.
(134) Wada, T.; Kishida, E.; Tomiie, Y.; Suga, H.; Seki, S.; Nitta, I. *Bull. Chem. Soc. Jpn.* **1960**, *33*, 1317−1318.
(135) Blake, A.; Ebsworth, E. A. V.; Welch, A. J. *Acta Crystallogr.* **1984**, *C40*, 413−415.
(136) Florencio, F.; Smith, P. *Acta Crystallogr.* **1970**, *B26*, 659−666.
(137) Jönsson, P.-G. *Acta Crystallogr.* **1971**, *B27*, 893−898.
(138) Housty, J.; Hospital, M. *Acta Crystallogr.* **1965**, *18*, 693−697.
(139) Bruno, G.; Randaccio, L. *Acta Crystallogr.* **1980**, *B36*, 1711−1712.
(140) Strieter, F. J.; Templeton, D. H. *Acta Crystallogr.* **1962**, *15*, 1240−1247.
(141) Nahringbauer, I. *Acta Crystallogr.* **1978**, *B34*, 315−318.
(142) Morrison, J. D.; Robertson, J. M. *J. Chem. Soc*. **1949**, 1001−1008.
(143) Puper, W. P. *Acta Crystallogr.* **1971**, *B27*, 344−348.
(144) Goedkoop, J. A.; MacGillavry, C. H. *Acta Crystallogr.* **1957**, *10*, 125−127.
(145) Derissen, J. L. *Acta Crystallogr.* **1970**, *B26*, 901−904.
(146) Derissen, J. L.; Smit, P. H. *Acta Crystallogr.* **1974**, *B30*, 2240−2242.
(147) Strieter, F. J.; Templeton, D. H.; Scheuerman, R. F.; Sass, R. L. *Acta Crystallogr.* **1962**, *15*, 1233−1239.
(148) Housty, P. J.; Hospital, M. *Acta Crystallogr.* **1966**, *20*, 325−329.
(149) Housty, P. J.; Hospital, M. *Acta Crystallogr.* **1965**, *18*, 753−755.
(150) Broadley, J. S.; Cruickshank, D. W. J.; Morrison, J. D.; Robertson, J. M.; Shearer, H. M. M. *Proc. R. Soc. London* **1959**, *A251*, 441−457.
(151) Scheuerman, R. F.; Sass, R. L. *Acta Crystallogr.* **1962**, *15*, 1244−1247.
(152) Margulis, T. N. *J. Am. Chem. Soc.* **1971**, *93*, 2193−2195.
(153) Lundén, B.-M. *Acta Crystallogr.* **1976**, *B32*, 3149−3153.
(154) Jeffrey, G. A.; Rosenstein, R. D.; Vlasse, M. *Acta Crystallogr.* **1967**, *22*, 725−733.
(155) Kroon, J.; Kanters, J. A. *Acta Crystallogr.* **1973**, *B29*, 1278−1283.
(156) Adams, J. M.; Morsi, S. E. *Acta Crystallogr.* **1976**, *B32*, 1345−1347.
(157) Busetti, V.; Del Pra, A.; Mammi, M. *Acta Crystallogr.* **1969**, *B25*, 1191−1194.
(158) Buschmann, J.; Müller, E.; Luger, P. *Acta Crystallogr.* **1986**, *C42*, 873−876.
(159) Watson, W. H.; Nagl, A. *Acta Crystallogr.* **1988**, *C44*, 1627−1629.
(160) André, D.; Fourme, R. *Acta Crystallogr.* **1972**, *B28*, 2389−2395.
(161) Luger, P.; Buschmann, J. *J. Am. Chem. Soc.* **1984**, *106*, 7118−7121.

(162) Van den Ham, D. M. W.; Van Hummel, G. J.; Huiszoon, C. *Acta Crystallogr.* **1978**, *B34*, 3134−3137.
(163) Dapporto, P.; Ghilardi, C. A.; Mealli, C.; Orlandini, A.; Pacinotti, S. *Acta Crystallogr.* **1984**, *C40*, 891−894.
(164) Merritt, L. L., Jr.; Schroeder, E. D. *Acta Crystallogr.* **1956**, *9*, 801−804.
(165) Johnson, J. E.; Jacobson, R. A. *Acta Crystallogr.* **1973**, *B29*, 1669−1674.
(166) Wheatley, P. J. *Acta Crystallogr.* **1960**, *13*, 80−85.
(167) Kravers, M. A.; Antipin, M. Y.; Struchkov, Y. T. *Cryst. Struct. Commun.* **1980**, *9*, 955−958.
(168) Alden, R. A.; Kraut, J.; Traylor, T. G. *J. Am. Chem. Soc.* **1968**, *90*, 74−82.
(169) Chaplot, S. L.; Lehner, N.; Pawley, G. S. *Acta Crystallogr.* **1982**, *B38*, 483−487.
(170) Bacon, G. E.; Curry, N. A.; Wilson, S. A. *Proc. R. Soc. London* **1964**, *279*, 98−110.
(171) Nijveldt, D.; Vos, A. *Acta Crystallogr.* **1988**, *B44*, 281−289.
(172) Trotter, J. *Acta Crystallogr.* **1961**, *14*, 1135−1140.
(173) Fawcett, J. K.; Trotter, J. *Proc. R. Soc. A* **1965**, *289*, 366−376.
(174) Prince, E.; Schroeder, L. W.; Rush, J. J. *Acta Crystallogr.* **1973**, *B29*, 184−191.
(175) van Nes, G. J. H.; Vos, A. *Acta Crystallogr. B* **1978**, *34*, 1947−1956.
(176) van Nes, G. J. H.; Vos, A. *Acta Crystallogr.* **1979**, *B35*, 2593−2601.
(177) Rao, S. T.; Sundaralingam, M. *Acta Crystallogr.* **1972**, *B28*, 694−699.
(178) Iverson, D. J.; Hunter, G.; Blount, J. F.; Damewood, J. R., Jr.; Mislow, K. *J. Am. Chem. Soc.* **1981**, *103*, 6073−6083.
(179) Brock, C. P.; Dunitz, J. D. *Acta Crystallogr.* **1982**, *B38*, 2218−2228.
(180) Norman, N.; Mathisen, H. *Acta Chem. Scand.* **1961**, *15*, 1755−1760.
(181) Mathisen, H.; Norman, N.; Pedersen, B. F. *Acta Chem. Scand.* **1967**, *21*, 127−135.
(182) Donaldson, D. M.; Robertson, J. M. *Proc. R. Soc. A* **1953**, *220*, 157−170.
(183) Camerman, A.; Trotter, J. *Proc. R. Soc. London* **1963**, *A279*, 129−146.
(184) Petricek, V.; Cisarova, I.; Hummel, L.; Kroupa, J.; Brezina, B. *Acta Crystallogr.* **1990**, *B46*, 830−832.
(185) Hazell, A. C.; Larsen, F. K.; Lehmann, M. S. *Acta Crystallogr.* **1972**, *B28*, 2977−2984.
(186) Baughman, R. H.; Kohler, B. E.; Levy, I. J.; Spangler, C. *Synth. Met.* **1985**, *11*, 37−52.
(187) Ahmed, F. R.; Trotter, J. *Acta Crystallogr.* **1963**, *16*, 503−508.
(188) Goodrow, M. H.; Musker, W. K.; Olmstead, M. M. *Acta Crystallogr.* **1986**, *C42*, 255−256.
(189) Valle, G.; Busetti, V.; Mammi, M.; Carazzolo, G. *Acta Crystallogr.* **1969**, *B25*, 1432−1436.
(190) DeSimone, R. E.; Glick, M. D. *J. Am. Chem. Soc.* **1976**, *98*, 762−767.
(191) Chan, T. L.; Mak, T. C. W. *Acta Crystallogr.* **1984**, *C40*, 1452−1454.
(192) Sekido, K.; Ono, H.; Noguchi, T.; Hirokawa, S. *Bull. Chem. Soc. Jpn.* **1977**, *50*, 3149−3152.
(193) Valle, G.; Busetti, V.; Mammi, M.; Carazzolo, G. *Acta Crystallogr.* **1969**, *25*, 1631−1636.
(194) Pfisterer, H.; Ziegler, M. L. *Acta Crystallogr.* **1983**, *C39*, 372−375.
(195) Sakai, T.; Taira, Z.; Ueji, S. *Acta Crystallogr.* **1987**, *C43*, 1156−1158.
(196) Fehér, F.; Engelen, B. *Acta Crystallogr.* **1979**, *B35*, 1853−1857.
(197) Lee, J. D.; Bryant, M. W. R. *Acta Crystallogr.* **1969**, *B25*, 2497−2504.
(198) Fehér, F.; Lex, J. *Z. Anorg. Allg. Chem.* **1976**, *423*, 103−111.
(199) Herbstein, F. H.; Ashkenazi, P.; Kaftory, M.; Kapon, M.; Reisner, G. M.; Ginsburg, D. *Acta Crystallogr.* **1986**, *B42*, 575−601.
(200) Rettig, S. J.; Trotter, J. *Acta Crystallogr.* **1987**, *C43*, 2260−2262.
(201) Kato, K. *Acta Crystallogr.* **1972**, *B28*, 606−610.
(202) Solans, X.; Font Altaba, M.; Pericas, M. A.; Riera, A. *Acta Crystallogr.* **1987**, *C43*, 1976−1978.